Journal of Cleaner Production 437 (2024) 140235

Contents lists available at ScienceDirect

Journal of Cleaner Production

journal homepage: www.elsevier.com/locate/jclepro

# Experimental results, integrated model validation, and economic aspects of agrivoltaic systems at northern latitudes

Pietro Elia Campana [a,*], Bengt Stridh [a], Torsten Hörndahl [b], Sven-Erik Svensson [b], Sebastian Zainali [a], Silvia Ma Lu [a], Tekai Eddine Khalil Zidane [a], Paolo De Luca [c], Stefano Amaducci [d], Michele Colauzzi [d]

[a] Mälardalen University, Department of Sustainable Energy Systems, Västerås, Sweden
[b] Swedish University of Agricultural Sciences, Department of Biosystems and Technology, Alnarp, Sweden
[c] Barcelona Supercomputing Center, Barcelona, Spain
[d] Università Cattolica del Sacro Cuore, Department of Sustainable Crop Production, Piacenza, Italy

A R T I C L E  I N F O

Handling Editor: Jin-Kuk Kim

*Keywords:*
Agrivoltaic
Soil moisture
Leaf area index
Integrated modelling
Shading
Validation
Profitability

A B S T R A C T

Agrivoltaic systems, which allow the coexistence of crop and electricity production on the same land, are an integrated water–energy–food nexus solution that allows the simultaneous attainment of conflicting Sustainable Development Goals. This study aims to analyse experimental results on the responses of ley grass yield and quality to shadings in the first agrivoltaic system in Sweden. It also aims to validate an integrated modelling platform for assessing agrivoltaic systems' performances before installation. An economic analysis is carried out to compare the profitability of agrivoltaic versus conventional ground-mounted photovoltaic systems and, using a Monte Carlo Analysis, to identify the parameters that most affect the profitability. Despite the agrivoltaic systems' supporting structures and photovoltaic modules producing an average ~25% reduction in photosynthetically active radiation at ground level, no statistically significant difference was observed between the yield of the samples under the agrivoltaic system compared to the yield of the samples in the reference area. The agrivoltaic system attained land equivalent ratios of 1.27 and 1.39 in 2021 and 2022, respectively. The validation results of the integrated modelling platform show that the sub-model concerning the crop yield response to shading conditions tends to underestimate ~7% the actual average crop yield under the agrivoltaic system. The results of the economic analysis show that, from a net present value perspective, agrivoltaic systems have a profitability that is ~30 times higher than a conventional crop rotation in Sweden.

## 1. Introduction

One of the main criticisms of large-scale conventional ground-mounted photovoltaic (CGMPV) systems built on agricultural land is that they compete with food production (Capellán-Pérez et al., 2017). The rivalry between land for energy and land for food is seen as a threat to food security, and it creates deep conflicts among the Sustainable Development Goals (SDGs) (i.e., Zero Hunger, Affordable and Clean Energy, and Climate Action) (Brunet et al., 2020). Applying the concept of agrivoltaic (APV) systems (see Fig. 1) can solve this conflict because agricultural crop production and green electricity production from PV systems can be synergistically combined.

Assuming the use of one reference hectare of land for installing an optimized CGMPV farm (Fig. 1, left), the output of the reference hectare will be defined as 100% electricity. This assumption does not consider other co-benefits produced by the solar farm, such as biodiversity or soil restoration, or the possibility to integrate livestock grazing. If the same hectare is used only for agriculture, the output will be defined as 100% crop production (Fig. 1 centre). Laws and regulations that protect food security may prohibit the reference hectare of land from being used for installing a conventional solar farm by, for instance, the authorities releasing project approvals or building permits. In such cases, a conflict arises between SDG 2 Zero Hunger, SDG 7 Affordable and Clean Energy, and SDG 13 Climate Action. This situation does not allow the attainment of multiple SDGs. For instance, according to the Swedish Environmental Code, agricultural land that is suitable for cultivation is of "national importance", and it cannot be exploited for other purposes unless it is to satisfy a significant national interest and no other land can be used

* Corresponding author.
*E-mail address:* pietro.campana@mdu.se (P.E. Campana).

https://doi.org/10.1016/j.jclepro.2023.140235
Received 31 July 2023; Received in revised form 11 December 2023; Accepted 15 December 2023
Available online 21 December 2023

(Chapter 3, Section 4) (The Swedish Government, 2000). In the APV scenario (Fig. 1, right), land can be used simultaneously for agricultural and PV production. The APV electricity supply is lower than an optimized CGMPV farm. This is because CGMPV aims at producing maximum energy with the lowest possible cost, which leads to high densities of PV modules per hectare. In contrast, an optimized APV sets a greater distance between adjacent rows to avoid excessive shading on crops. This lowers the density of PV modules per hectare, i.e., X% PV electricity production in Fig. 1 is lower than 100%. The crop output depends on the APV configuration, such as the PV module density per hectare and related shading levels, the geographical location of the system, specific weather conditions, and crop type. The yield Y% can be lower or higher than the crop yield in the reference agricultural land, i.e., Y% crop production can be lower or higher than 100% (Laub et al., 2021). A typical example of crop production being higher under an APV system is connected to installations in arid or semi-arid regions (Barron-Gafford et al., 2019). Higher crop yields under APV systems might be obtained during the occurrence of extreme weather phenomena such as drought thanks to the shade reducing water and heat stresses on crops (Trommsdorff et al., 2021).

In addition to crop production and electricity production, APV systems present other benefits. Agostini et al. (2021) qualitatively assessed the impacts that the Agrovoltaico® system (a patented APV configuration) has on SDGs and identified that the APV system could positively impact 14 out of 17 SDGs. For instance, as compared to agriculture alone, the presence of PV modules creating shadings affects the energy balance at the ground and crops level, thereby reducing evapotranspiration and, thus, water loss from soils and crops (Elamri et al., 2018) (i.e., SDG 6 Clean Water and Sanitation). Reduced evapotranspiration can significantly benefit areas with high water-stress indices. At the same time, APV systems offer an opportunity for farmers in terms of revenues, since the same reference area can produce two streams of revenues, i.e., revenues from electricity production and crop production. The higher value of electricity income compared to crop income, especially for conventional crop rotations and without subsidies, can lead to higher specific income (i.e., €/m$^2$) for farmers. The specific profit per area can also be increased by leasing the land to a third-party company, which directly invests in the APV system and pays annual rent on the land. Moreover, combining PV and crop production can also lead to more stable revenues, especially from the crop production stream, since shading reduces the shocks that extreme weather phenomena such as droughts cause to crop yields (Dietz et al., 2021). The positive economic aspects connected to the implementation of APV systems are pivotal for small-holder farms (which are typically marked out by poorer economies compared to large-scale industrial farms) and more broadly for the economic development in rural areas (i.e., SDG 8, Decent Work and Economic Growth).

On the other hand, APV systems present several challenges, such as their uneven distribution of precipitation, soil erosion (Verheijen and Bastos, 2023) and the general risk of decreasing agricultural production. Crop yield can be reduced under APV systems due to less light reaching the crops because of shade from the PV modules. A fundamental step is thus to design the APV system to maximize both crop yield and electricity production, despite those objectives being in mutual conflict (Campana et al., 2021). Typical parameters to be considered are shade level, crops' shade tolerance, water stress coefficients, the need for irrigation, crop rotation during the lifetime of the APV system, and the increased cost of farming the land between the PV system. The crop yield reduction under the APV system is typically considered a crucial key performance indicator for meeting policy requirements. In countries where APV systems have been implemented for several years – or at least where research activities have been active for a long time – legislators have provided definitions of APV systems and have identified clear policy targets. For instance, those APV policy targets focus on maximum thresholds for the reduction in crop yield under APV systems or the maximum area that can be covered by PV modules. To cite some, in Germany, the law sets the maximum crop yield reduction under an APV system at 34% (European Standards, 2023). In Italy, an APV system must have a PV module area coverage of less than 40%. At the same time, the continuity of agricultural activities should be guaranteed (Italian Ministry of the Environment and Energy Security, 2023). The Japanese legislation defines crop yield under an APV system as at least 80% compared to the yield in open-field conditions (Gonocruz et al., 2022).

It is fundamental to have integrated tools that estimate crop yield reduction under APV systems before installation to meet policy targets. As compared to the studies by Campana et al. (2021, 2022a), which focused on the development of the integrated modelling platform for simulations and optimization of APV systems, this study aims to analyse crop performance under an APV system and validate the integrated modelling platform with special consideration of crop model calibration and validation. The integrated modelling platform combines cutting-edge PV models for bifacial PV modules, shading models on the ground and PV array, microclimate models, and crop models to study the interactions between shading and microclimate and between microclimate and crop yield. The validation is carried out using data from the research activities conducted on the first APV system at Kärrbo Prästgård in Sweden using ley grass as a crop. This study also summarizes the performance of APV systems in terms of crop adaption and soil moisture and Land Equivalent Ratio (LER) and provides insights into the economic performances of APV systems compared to CGMPV systems and agriculture. To the best of the authors' knowledge, this study is one of the first studies on validating an integrated modelling platform for APV systems and it is one of the first experimental studies on the integration of APV systems at northerly latitudes.

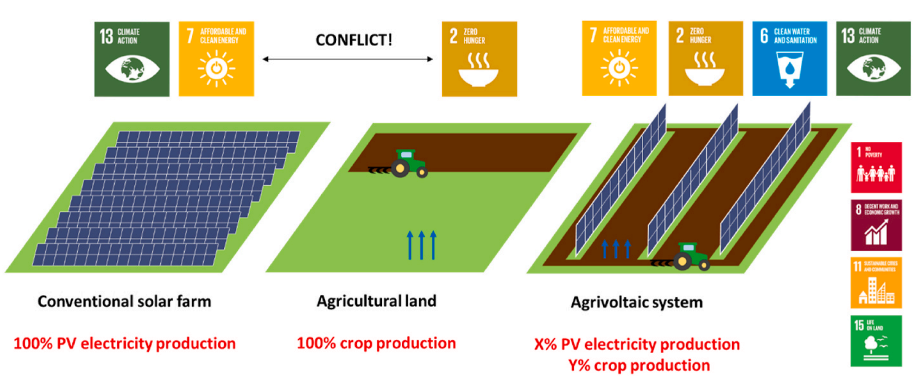


**Fig. 1.** Land use conflicts between conventional solar farms and agriculture, and how these conflicts can be relieved by implementing APV systems in the context of Sustainable Development Goals. Adapted from Fraunhofer ISE (2023)

## 2. Background

In 2022, according to Al Mamun et al. (2022), Sweden's first APV system was the world's northernmost APV research system. The decision to conduct research activities on APV systems in Sweden was driven by research on minimizing irrigation water requirements during drought conditions (Campana et al., 2018, 2022b). Further motivations of the project were to avoid the conflicts between food production and solar parks and provide better incomes for farmers.

In 2020, at the beginning of the first APV project in Sweden, the utility-scale CGMPV systems represented a relatively new market segment, with a share of about 7% of the total PV market (Lindahl et al., 2022). Nevertheless, although unsubsidized in the last three years, the market for CGMPV systems has grown significantly due to several factors. These include utility-scale PV systems reaching grid parity (i.e., the cost of electricity from PV has reached the same level of conventional power sources) and increasing spot market electricity prices. Despite being a new market segment and the availability of land in Sweden, the rapid interest in utility-scale CGMPV systems has encountered resistance from some Country Administrative Boards (the entities releasing the projects approval) due to the competition between food production and energy conversion (Nordiskaprojekt, 2023). In this context, APV systems can represent an intelligent solution to preserve food production while simultaneously allowing the attainment of renewable energy and electrification targets. Currently, no definition and guidelines for APV systems exist in Sweden. To the best knowledge of the authors, no previous experimental activities at high latitudes or in Sweden have been reported on APV systems before this study.

Integrated tools for APV applications typically combine algorithms for PV system electricity production, microclimates produced by shadings, and crop growth. Weselek et al. (2019) highlighted that one of the major knowledge gaps in APV research is how the technology affects crop yield and quality. In this context, the authors also highlighted that integrated modelling is one of the directions to follow towards developing universal models that can be validated through specific experiments but that then provide robust results when applied to different climate conditions and crops. Dupraz et al. (2011) and Dinesh and Pearce (2016) predicted crop yield under APV systems using computer software such as the STICS (Simulateur mulTIdisciplinaire pour les Cultures Standard) (STICS, 2023) developed in France (Brisson et al., 2003). Amaducci et al. (2018) used GECROS v3.0 to obtain leaf temperature, photosynthesis, transpiration and crop yield under APV systems. Elamri et al. (2018) used the software AVirrig to assess the impact of fluctuating shadings on crop growth (by assuming stomatal conductance as a relevant variable) to help with scheduling irrigation. Campana et al. (2021) integrated the Environmental Policy Impact Climate (EPIC) crop model (Williams et al., 1989) in the open-source package OptiCE (Campana et al., 2017; OptiCE, 2023) for electricity modelling of PV systems to study the effects that shadings beneath APV systems had on oats and potatoes. Mengi et al. (2023) developed a model to simulate solar irradiation distribution under APV systems and feed those inputs into the SIMPLE crop model (Zhao et al., 2019) to analyse the effects of shadings on biomass accumulation, as compared to open-field conditions. The SIMPLE crop model simulates crop growth using a simplified approach based upon a few functions. To reduce the complexity of using advanced crop models, several authors have used the light-response curve concept that describes the relationships between incoming photosynthetically active radiation (PAR) and photosynthetic rate. Yajima et al. (2023) used the photosynthetic rate equation derived by Sugimoto (2001) to study the effects of PV modules shading on taro cultivation in Japan. Katsikogiannis et al. (2022) used the light response curve of highbush blueberry leaf from Li et al. (2012) to estimate the effects of shading from several APV system configurations on PAR reduction and net $CO_2$ assimilation rate. Other authors have instead used empirical approaches that employ equations that correlate the shading rate to crop yield. Riaz et al. (2021) adopted an empirical model that correlates the crop yield under the APV system to the ground coverage ratio and crop yield in open-field conditions. Willockx et al. (2023) fitted the data from Artru et al. (2018) to develop a relationship between shading level and radiation use efficiency for sugar beet cultivation in Belgium. There are several research studies that report crop yield performances under APV systems. For instance, Weselek et al. (2021) reported the difference in yield for four different crops, (i.e., celeriac, winter wheat, potato, and grass-clover) under APV systems versus open-field conditions. Gonocruz et al. (2021) reported rice yields for different shading rates produced by APV systems in Japan. AL-agele et al. (2021) investigated tomato yield under different shading and irrigation conditions in an experimental APV system in the USA.

From the literature review, there is a clear trend in developing modelling tools that can simulate the effects of shadings on microclimate and crop production. Nevertheless, there is a general lack of studies focusing on the validation of those models, especially microclimate and crop models. One of the few studies carried out on this aspect is the work carried out by Potenza et al. (2022), where the integrated modelling platform by Amaducci et al. (2018) was validated for soybean cultivated under a stilt-mounted APV system with two-axis trackers in Italy. This study fills two research gaps. The first concerns the validation of integrated modelling platforms for assessing APV system performances with special focus on crop modelling. The second is how APV systems at northerly latitudes perform in terms of crop yield response under shading conditions.

The remainder of the paper is organized as follows: Section 3 describes the siting and the principal characteristics of the APV experimental facility, the crop experiments, the integrated modelling platform development, and the economic model for APV systems; Section 4 presents the main results of the study in terms of an integrated APV modelling platform with particular focus on crop model validation, and the results of the techno-economic analyses; Section 5 summarizes the conclusions of the study.

## 3. Methods

### 3.1. Siting and experimental facility description

The siting for the APV system experimental facility was performed in early 2021 by analysing differences in crop yield and chemical composition for a selected field within a farm located nearby Västerås, Sweden: Kärrbo Prästgård (59.5544N, 16.7534E). The siting aimed to identify a plot with uniform vegetation. This task was performed using CropSAT (2023), a tool that visualizes crop variation within fields using satellite images post-processed to produce a vegetation index. The vegetation depicts the relationship between infrared and red light reflected from the foliage and correlates it to the crop biomass content (Söderström et al., 2017). CropSAT is based on satellite images retrieved from the Sentinel-2 and Landsat 8 satellites, and it was evaluated and proven to give satisfactory results by Söderström et al. (2015). The vegetation index was retrieved for five dates during the crop growing season in 2020, i.e., before the actual installation of the APV system facility, and is presented in Fig. 2. The colour scheme shows that yellow grids correspond to in-field sites with the lowest biomass level, while dark green grids correspond to in-field areas with the highest biomass level. The APV system facility includes the vertically mounted APV system, the reference area, and the CGMPV system for intercomparison.

The APV system is designed with vertically mounted bifacial PV modules installed in a quasi north–south direction, with a row-to-row distance of 10 m, to facilitate the harvest. The APV system capacity is 22.8 $kW_p$. The PV system comprises 60 bifacial PV modules arranged in three rows of 17.9 m in length. The APV system is compared to a reference system built as a CGMPV system of 11.8 $kW_p$, which comprises 32 bifacial PV modules arranged in two rows 8.6 m long and with a tilt angle of 30°. Fig. 3 shows the APV system while performing the first cut in 2021, with the CGMPV system in the background. The system

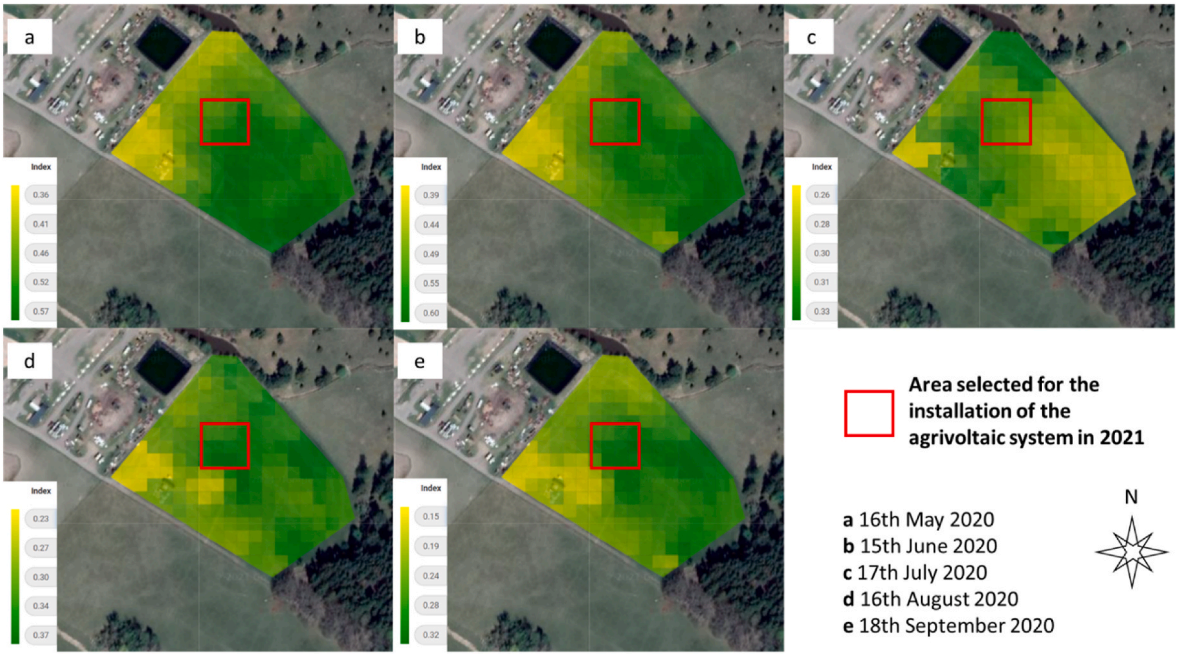


**Fig. 2.** Site selection based on satellite images processed in CropSAT (2023).

**Fig. 3.** Vertically mounted APV system during the first cut in 2021 and reference CGMPV system in the background.

configuration takes inspiration from the experimental setup presented by Barron-Gafford et al. (2019). A summary of the characteristic parameters of the APV and reference CGMPV systems is provided in Table 1. At the end of 2022, the experimental facility was monitored with more than 20 sensors for weather, microclimate, power, and agricultural parameters. A schematic diagram of the monitoring system is presented in Fig. 4.

### *3.2. Crop experiments*

#### *3.2.1. Crop biomass yield and nutrient content*

The APV experimental facility is built on a field that has been in grass production for several years. Most crop species are grasses, but there are also a wide variety of legumes and herbs, most of which are perennial plants. Hereafter, we will refer to the crop as "ley grass". The farm owner maintains the ley grass field with an organic farming approach.

In 2021, to study the influence of shading from the PV modules, both for the APV system and CGMPV system, thirty squares (each 0.25 m$^2$) were distributed in six groups of five plots, as depicted in Fig. 5. "Group A" corresponds to samples 1–5, "group B" to samples 6–10, "group C" to samples 11–15, "group D" to samples 16–20, "group E" to samples 21–25, and "group R" to samples 26–30. The distances between APV system, reference area, and CGMPV system are also provided in Fig. 5. The distance between the APV system and the reference area was estimated through accurate shading analyses to avoid shading on the

**Table 1**
Summary of the characteristic parameters of the APV and reference CGMPV systems.

| | APV | Reference CGMPV |
|---|---|---|
| Azimuth angle (°) | −84 | 6 |
| Tilt angle (°) | 90 | 30 |
| Power (kW$_p$) | 22.8 | 11.8 |
| Number of strings | 2 | 2 |
| Row-to-row distance | 10 | 9.1 |
| | **PV modules** | |
| Manufacturer | Jolywood | Longi |
| Model | JW-D72N-380 | LR4-60HBD-370 M |
| Type | Bifacial, mono | Bifacial, mono |
| $P_{mp}$ ($W_p$) | 380 | 370 |
| $I_{mp}$ (A) | 9.44 | 10.79 |
| $V_{mp}$ (V) | 40.2 | 34.3 |
| $I_{sc}$ (A) | 9.93 | 11.50 |
| $V_{oc}$ (V) | 49.5 | 40.9 |
| Length (m) | 1.974 | 1.755 |
| Width (m) | 0.992 | 1.038 |
| Module efficiency (%) | 19.4 | 20.3 |
| Front side efficiency (%) | 19.4 | – |
| Back side efficiency (%) | 16.5 | – |
| Temperature coefficient of max power (%/°C) | −0.38 | −0.35 |
| | Inverter | |
| Manufacturer | SunGrow | SunGrow |
| Model | SG20RT | SG15 KTL-M |
| AC Power (kW) | 20 | 15 |
| Max efficiency (%) | 98.4 | 98.6 |
| Euro efficiency (%) | 97.4 | 98.3 |
| MPP inputs | 2 | 2 |

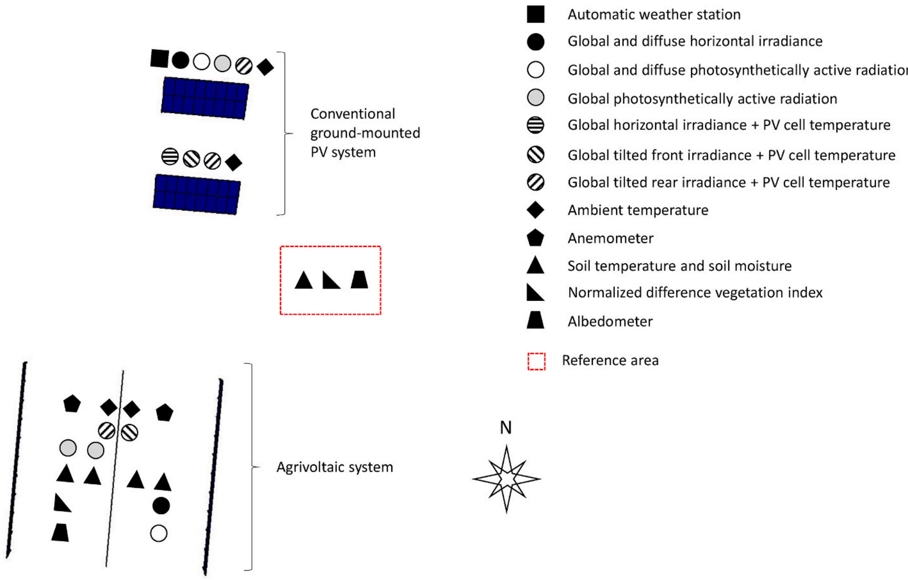


**Fig. 4.** Schematic diagram of the experimental facility and sensors integrated at the end of 2022.

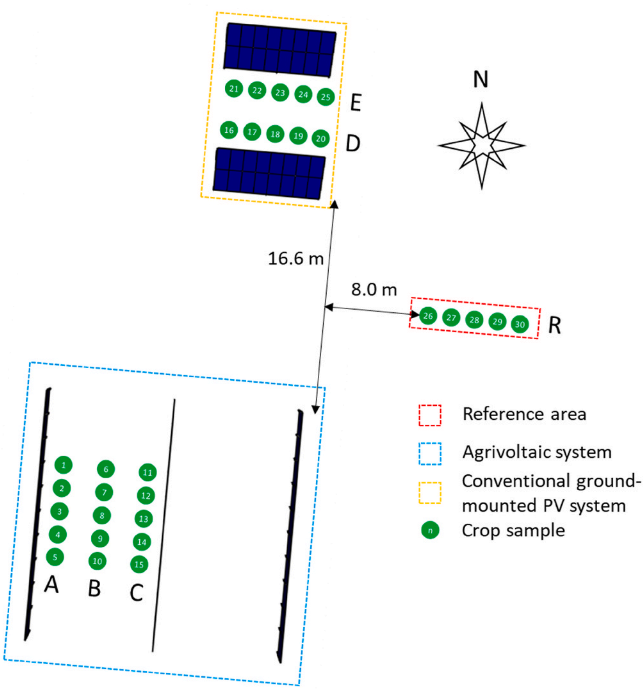


**Fig. 5.** Crop yield experiment layout in 2021.

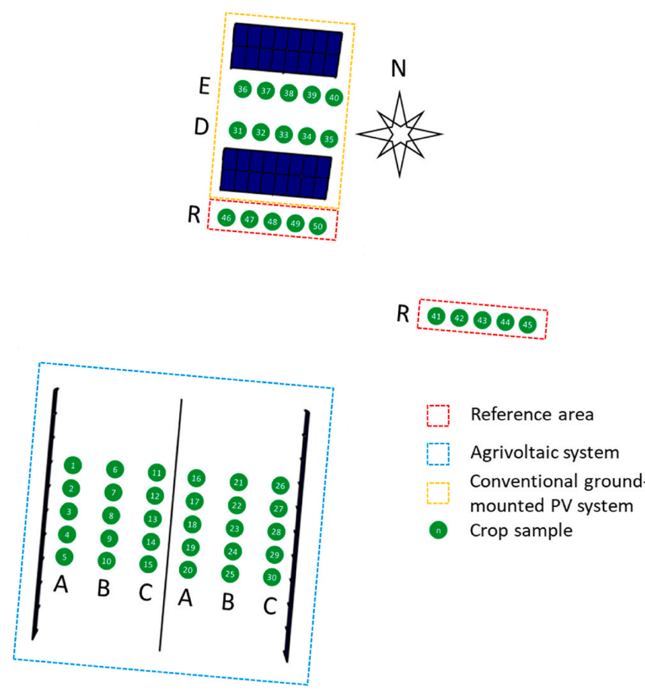


**Fig. 6.** Crop yield experiment layout in 2022.

reference area. In 2021, the reference area for monitoring the differences in crop yield under the APV system and the reference CGMPV system was located on the east side of the installation. In 2022, fifty squares (each 0.25 m$^2$) were distributed in six groups of five/ten plots, as shown in Fig. 6. "Group A" corresponds to samples 1–5 and 16–20, "group B" to samples 6–10 and 21–25, "group C" to samples 11–15 and 26–30, "group D" to samples 31–35, "group E" to samples 36–40, and "group R" to samples 41–50. Thirty squares had the same position as in 2021. The other twenty squares were distributed in four groups of five plots to study more in-depth the plots in the same position as groups A, B, C and R. Thus, in 2022, there were four groups with ten plots (A, B, C, and R) and two groups with five plots (D and E).

Figs. 5 and 6 also include the samples' reference numbers. In 2022, the reference area was located on the east side of the installation and in front of the CGMPV system.

In 2021, in correspondence with the samples in groups A (1–5), B (6–10), C (11–15), and R (26–30) of Fig. 5, soil samples were taken to analyse the type of soil. The chemical characteristics of the soil show typical values for soil with a high clay content that has been used to cultivate ley grass for several years. The only notable point is that assimilable phosphorous is much lower in sample group C than in the other groups. For more detailed information, see Table A1 in the Appendix.

In 2022, a botanical analysis was performed by analysing the percentage content of the following components: "grass", "legumes", and "other". In Fig. 7, the average distribution is presented. About 50% of

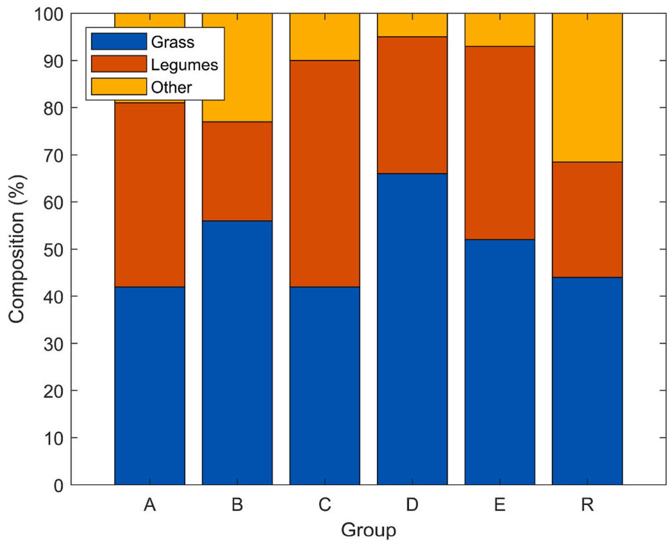


**Fig. 7.** Botanical analysis carried out the July 14, 2022 (second cut).

the botanical composition is grass, but for groups A and C is only ~40%, while D has 66%. The content of legumes is, on average ~34%. The analysis for group B showed the lowest content of legumes at 21%, while groups C and E showed the highest content at 48% and 43%, respectively. The different species of plants in the groups are not determined, so it is impossible to know the effect of this difference.

In 2021, no additional nutrients were supplied to the ley grass. The crop depended on mineralization from the soil and air assimilation. The farm owner spread solid manure from cattle in 2020. To minimize the effect of nutrient deficiency, in 2022, a necessary amount of N, P, and K were distributed to the plots, as summarized in Table 2.

In the statistical analysis, the yield, energy, and protein content, for the three harvests during the year were used as a response. Given the layout of the experiments, the statistical analyses were performed as a balanced one-way ANOVA with five replicates during 2021 and an unbalanced one-way ANOVA with five and ten replicates during 2022.

The plots were hand-harvested to determine the biomass yield and nutrient content, such as crude protein and energy content. The grass samples were dried for 24 h at 60 °C and weighed to determine the dry matter (DM) (%) and total crop yield (kg of DM/ha) (Åkerlind et al., 2011). The chemical analysis was performed by further drying and milling the grass samples to estimate the ash content, the nitrogen content by the Kjeldahl method, and the metabolizable energy (ME) through 96 h *in-vitro* digestibility using standard methods (Volden and Nielsen, 2011).

#### 3.2.2. Soil moisture

In 2021, data concerning soil moisture at the reference plot and under the APV system were available for only part of the season due to sensors having failed during a thunderstorm at the end of July. Campbell Scientific CS655 soil moisture sensors were installed at 10 cm depth in groups A, B, C, and R. In 2022, the soil moisture campaign was strengthened by installing four Truebner SMT50 soil moisture sensors at group R. Three moisture sensors were installed at 10 cm depth, while one soil moisture sensor was installed at 20 cm depth. Four Truebner SMT50 soil moisture sensors with a layout like group R were installed in groups B and C.

**Table 2**
Amount of fertilizer, presented as pure N, P, and K given to the plots in 2022.

| | N (g/m$^2$) | P (g/m$^2$) | K (g/m$^2$) |
|---|---|---|---|
| First cut | 5.8 | 1.4 | 2.9 |
| Second cut | 4.0 | 1.0 | 2.0 |
| Third cut | 2.0 | 0.5 | 1.0 |

#### 3.2.3. Leaf area index

The leaf area index (LAI) is one of the crop morphology traits most influenced by shading conditions (Potenza et al., 2022). LAI measurements were carried out in 2022 with a SunScan Canopy Analysis System – SS1, to study the crop adaption mechanisms under shading conditions. Six measurement campaigns for groups A–C and R were performed, with five replicates for each measurement.

### 3.3. Integrated modelling and optimization

The model developed by Campana et al. (2021, 2022a) has been employed in this study to simulate the effects of shadings on crop yield. The model has at its core the shading model that calculates both shadings on the ground and PV modules. The shading model is a modified version of the one presented by Cascone et al. (2011) and Melo et al. (2013). The shadings on the ground are used as a starting point to calculate the GHI, PAR, and diffuse PAR reaching the crop. PAR is retrieved from Strång (2023), while the decomposition of PAR into PAR diffuse is performed with the model by Starke et al. (2018) adapted for PAR decomposition, as one of the best performing models tested by Ma Lu et al. (2022). The computation of the shading is the starting point for calculating other microclimatic variables, such as ground temperature (Remund et al., 2018), evapotranspiration (Allen et al., 1998), and soil moisture distribution (Allen et al., 1998).

The irradiance model calculates the solar irradiance on the tilted surfaces of the bifacial modules. It is based on the studies carried out by Martín and Ruiz (2005), Khan et al. (2017), and Sun et al. (2018). The solar irradiance is converted into electricity through the five-parameter, single-diode model described by Duffie and Beckman (2013). The microclimate variables at crop level are fed into the EPIC crop model (Williams et al., 1989) that calculates potential biomass growth, growth stresses, and crop yield (Wang et al., 2022).

Since the sub-model for energy performances has been cross-validated in Campana et al. (2021) with a commercial software, and given that other parallel studies are investigating the energy aspects of the APV system and validation of the energy sub-model with actual measurements (Ma Lu et al., 2023; Zainali et al., 2023a), this study only focuses on the validation of the sub-model for crop response to shading. The methodology applied is the following: 1) the crop model parameters for ley grass were retrieved from crop databases such as those available in EPIC (Williams et al., 1989) and literature. Some of the key crop parameters are summarized in Table 3; 2) the crop model was calibrated with crop yield measurements from the reference area; 3) the calibrated

**Table 3**
Ley grass crop parameters for model initialization.

| Parameter | Value | Comment/Reference |
|---|---|---|
| Harvest index | 0.7 | Schils et al. (2013) |
| Biomass–energy ratio (kg/ha)/(MJ/m$^2$) | 24 | Derived from Schils et al. (2013) |
| Base temperature (°C) | 3 | Derived from Kiniry et al. (1995) |
| Optimal temperature (°C) | 20 | Derived from Kiniry et al. (1995) |
| Maximum LAI (m$^2$/m$^2$) | 5 | Derived from Schils et al. (2013) |
| Water stress-yield factor | 0.01 | Derived from Williams et al. (1989) |
| LAI declining factor | 1.5 | Derived from Kiniry et al. (1995) |
| Fraction of growing season when leaf area declines | 0.85 | Derived from Kiniry et al. (1995) |
| First point on optimal leaf area development curve | 40 | Derived from Kiniry et al. (1995) |
| Second point on optimal leaf area development curve | 70 | Derived from Kiniry et al. (1995) |
| Fraction of root weight at maturity | 0.2 | Derived from Williams et al. (1989) |

model was then fed with the microclimatic conditions of the APV system with a similar approach as in Campana et al. (2022a) to simulate the effect that the shading and microclimate produced by shadings had on the crop yield; 4) crop adaptation measurements such as LAI development under shading conditions were fed into the model to simulate the effects of shadings and microclimate on the crop yield as well as the effects of shadings on crop morphogenesis. The model calibration was performed by minimizing the Root Mean Square Error (RMSE) between measured ($y_m$ [t/ha]) and simulated ($y_s$ [t/ha]) crop yield in open-field conditions at each cut with an approach like Campana et al. (2022b). The optimization function is the following:

$$\min_x f(x), f(x) = RMSE = \sqrt{\frac{1}{n}\sum_{i=1}^{n}\left(y_{s,i} - y_{m,i}\right)^2}, \tag{1}$$

where, $n$ is the number of cuts, $y_{s,i}$ is the simulated yield for the $i$-th cut, and $y_{m,i}$ is the measured yield for the $i$-th cut. The optimization model uses as its algorithm a variant of Non-dominated Sorting Genetic Algorithm II (NSGA-II) (Deb et al., 2000) available in the Matlab® Global Optimization Toolbox. The decisional variables $x$ of the optimization model are the key parameters defining the biomass production and LAI curve development. Those parameters and their corresponding lower and upper boundaries are summarized in Table 4.

As pointed out by Schils et al. (2013), the biomass–energy ratio is relatively stable during the crop growing season but might decrease in the last stage of the growth. Thus, a more advanced optimization is run, adding a dedicated biomass–energy ratio for the last cut of the ley grass as a further decisional variable.

### 3.4. Economic analysis

In APV systems, several business models can exist because multiple actors can provide different functions, such as the provision of the land for the installation of the system, agricultural management, APV system installation, and PV system operation (Gorjian and Campana, 2022; Trommsdorff et al., 2022). To tackle this multitude of business models and the related economic aspects, we have developed a tool that can be adapted to different actors to analyse the profitability of APV systems. It can be requested from the authors.

In the economic analysis, a case where the landowner owns a commercial-scale APV system built on 0.2 ha has been analysed. We have assumed a permanent crop and a cropping system for the agricultural part of the APV system. In the former, the APV system is combined with permanent ley grass, while in the latter, it is combined with a conventional crop rotation as follows: barley, ley grass, ley grass, winter rape seed, winter wheat, and winter wheat (Tidåker et al., 2016). The annual profit given by the selected crops for a medium to high-yield configuration has been retrieved from Rosenqvist (2019). EU direct support for farmers accounts for about 150 €/ha/year plus 15.4 €/ha/year for the first 150 ha that receives support (Swedish Board of Agriculture, 2023). We have investigated and compared three scenarios, i.e., APV, CGMPV, and only agriculture. A case is added in which the landowner is not the actual owner of the APV system but leases the land to a third-party company. It must be noted that, for the APV scenario, although agriculture can coexist with electricity production, farmers currently cannot receive direct EU support (Scania County Administrative Board, 2023). The tool calculates the net present value (NPV) and the Discounted Payback Period (DPBP) of the project, which are defined as follows:

**Table 4**
Lower and upper boundaries for the crop model calibration.

| Parameter | Value | Comment/Reference |
|---|---|---|
| Harvest index | 0.7 ± 25% | Assumption derived from Schils et al. (2013) |
| Biomass–energy ratio (kg/ha)/(MJ/m$^2$) | 10–40 | Derived from Schils et al. (2013) |
| Base temperature (°C) | 0–4 | Derived from Kiniry et al. (1995) and Williams et al. (1989) |
| Optimal temperature (°C) | 15–25 | Derived from Kiniry et al. (1995) and Williams et al. (1989) |
| Maximum LAI (m$^2$/m$^2$) | 4–6 | Schils et al. (2013) |
| LAI declining factor | 1–2 | Derived from Kiniry et al. (1995) |
| First point on optimal leaf area development curve | 35–50 | Derived from Kiniry et al. (1995) |
| Second point on optimal leaf area development curve | 60–90 | Derived from Kiniry et al. (1995) |

$$NPV = -ICC + \sum_{y=1}^{N}\frac{CF_y}{(1+d)^y}, \tag{2}$$

$$DPBP = Y_{DCCF>0} - 1 + \frac{\left|DCCF_{t=(Y_{DCCF>0}-1)}\right|}{DCF_{t=(Y_{DCCF>0})}} \tag{3}$$

where, $ICC$ is the initial capital cost (Euro [€]), $N$ is the lifetime of the project (years), $CF_y$ is the cash flow in the $y$-th year (€), $d$ is the real discount rate (%), $DCCF$ is the discounted cumulative cash flow (€), $Y_{DCCF>0}$ is the first year at which the DCCF (€) is greater than 0, and $DCF$ is the discounted cash flow (€). The $ICC$ is calculated as a product of the installed capacity times the specific cost (i.e., €/kW$_p$). The revenues generated by the system are given by the profit of the agricultural production (i.e., annual profit [€/ha] and the influence of PV modules on crop yield and annual profit [%]) and electricity sale or self-consumption. The costs of the system are associated with installation, operation and maintenance, replacements, and decommissioning. The operation and maintenance costs are assumed as 1% of the $ICC$ occurring each year (value derived from Lindahl et al. [2022]). We have assumed inverter replacements in the 17th year, costing 55 €/kW$_p$ (Lindahl et al., 2022). Decommissioning costs, depreciation, and salvage values were omitted in this study, as in Lindahl et al. (2022). The main technical and economic input data for the reference CGMPV system and APV system can be found in Table 5. For converting between Swedish Krona (SEK) and Euro (EUR [€]), we have assumed the average exchange rate in 2022 that was 0.0941 EUR/SEK (Exchange Rates UK, 2023).

Given the uncertainty of several parameters, a Monte Carlo Analysis is carried out for the APV system built on a 0.2 ha plot owned by the landowner by varying the sensitive parameters listed in Table 6, assuming a normal (Gaussian) distribution. To further analyse the impact of the sensitive parameters on the NPV, the Pearson's correlation coefficient (PCC) is calculated. While calculating the PCC, to understand the effect of the agronomic part on the NPV of the project, we have assumed the 30-year average crop profit for the crop rotation.

## 4. Results and discussions

### 4.1. Crop experiments

#### 4.1.1. Crop yield

In the 2021 season, the harvesting dates were June 1 (first cut), July 20 (second cut), and September 17 (third cut). In May, before the first cut, the total precipitation was 119 mm. Between the first and second cuts, the precipitation was 71 mm, while between the second and third cuts, it was 201 mm (SMHI, 2023). According to the Swedish Meteorological and Hydrological Institute (SMHI) data for Västerås, as presented in Table 7, May and August 2021 had over 50% more precipitation than the reference period (1990–2010), June was drier, and July was average (SMHI, 2023). In the 2022 season, the harvesting dates were June 3 (first cut), July 14 (second cut), and August 26 (third cut). In May, before the first cut, the precipitation was 69 mm. Between the first and second cuts, the precipitation was 52 mm, while between the second and third cuts, 61 mm was measured (SMHI, 2023). In 2022, May and August had more rain than the reference period (1990–2010), while June and July had lower precipitation than the reference period,

**Table 5**
Summary of the technical and economic input data.

| | Reference CGMPV | APV | Comment/Reference |
|---|---|---|---|
| Total ground net area (ha) | 0.2 | 0.2 | Assumed |
| PV system capacity ($kW_p$) | 150 | 84 | For the reference CGMPV system, we have assumed that 11.8 $kW_p$ covers a net area of 8.6m*18.2m. For the APV system, we have assumed that 22.8 $kW_p$ cover a net area of 30m*17.9m. Those geometries refer to the net area of the systems described in Table 1. |
| Area loss due to supporting structure (%) | 45 | 10 | For the reference CGMPV system, we have assumed that 11.8 $kW_p$ covers a net area of 8.6m*18.2 m. The PV modules of one row cover an area of 8.6m*3.1m. An extra 1 m is added as a clearance distance for agricultural machinery. For the APV system, a 10% loss due to the structure was assumed as in Campana et al. (2021). |
| Electricity production ($kWh/kW_p/1^{st}$ year) | 1116 | 1067 | Based on simulations of the PV system with bifacial modules with OptiCE. |
| System degradation rate (%/year) | 0.2 | 0.2 | Lindahl et al. (2022) |
| PV system specific cost (€/$kW_p$) | 880 | 940 | For the reference CGMPV, 880 €/$kW_p$ relates to 9380 SEK/$kW_p$, which was the average price for commercial projects in the order of 100–255 $kW_p$ in Lindahl et al. (2022). For the APV system, 940 €/$kW_p$ relates to 10,000 SEK/$kW_p$. Those values were used based on quotations for vertically mounted APV system projects. |
| Operation and maintenance (% system cost/year) | 1 | 1 | Derived from Lindahl et al. (2022) |
| Invert replacement costs (€/$kW_p$) | 55 | 55 | 55 €/$kW_p$ relates to 582 SEK/$kW_p$ occurring at the 17th year as assumed in Lindahl et al. (2022). |
| Decommissioning costs (% system cost) | 0 | 0 | Lindahl et al. (2022) |
| Electricity selling price (€/kWh) | 0.07 | 0.07 | 0.07 €/kWh relates to 0.76 SEK/kWh, which was the average electricity price during the period 2020–22 in the price area SE3 (Nord Pool, 2023). |
| Electricity buying price (€/kWh) | 0 | 0 | We assumed 0% self-consumption while comparing the APV system with the CGMPV system. In Table 6 and section 4.5, we have investigated the effect of the self-consumption on the APV system built on 0.2 ha land. |
| Self-consumption (%/year) | 0 | 0 | This value can be changed depending on the actor and business model adopted, and simulations or measured data. |
| Salvage value (% of system initial capital cost) | 0 | 0 | Lindahl et al. (2022) |
| Real discount rate (%) | 1.4 | 1.4 | Lindahl et al. (2022) |
| Annual profit ley grass (€/ha) | – | −151 | −151 €/ha relates to −1608 SEK/ha from Rosenqvist (2019). It refers to values classified as "medium to high yield". |
| Annual profit barley (€/ha) | – | 95 | 95 €/ha relates to 1012 SEK/ha from Rosenqvist (2019). It refers to values classified as "medium to high yield". |
| Annual profit winter rape seed (€/ha) | – | 262 | 262 €/ha relates to 2791 SEK/ha from Rosenqvist (2019). It refers to values classified as "medium to high yield". |
| Annual profit winter wheat (€/ha) | – | 371 | 371 €/ha relates to 3948 SEK/ha from Rosenqvist (2019). It refers to values classified as "medium to high yield". |
| EU direct support for farmers accounts for about (€/ha/year) | – | 150 + 15.4 | Swedish Board of Agriculture (2023) |
| Land lease (€/ha/year) | | 850 | Dagens Industry (2021) |

**Table 6**
Sensitive parameters of the Monte Carlo Analysis.

| Sensitive parameter | Mean value | Standard deviation | Comment |
|---|---|---|---|
| Specific electricity production ($kWh/kW_p/1^{st}$ year) | 1067 | 105 | The standard deviation is assumed to be 10% of the mean value. |
| PV system specific cost (€/$kW_p$) | 940 | 188 | The standard deviation is assumed to be 20% of the mean value. |
| Operation and maintenance (% system cost/year) | 1 | 0.2 | The standard deviation is assumed to be 20% of the mean value. |
| Inverter replacement (€/$kW_p$) | 55 | 11 | The standard deviation is assumed to be 20% of the mean value. |
| Electricity selling price (€/kWh) | 0.07 | 0.014 | The standard deviation is assumed to be 20% of the mean value. |
| Electricity buying price (€/kWh) | 0.14 | 0.028 | The standard deviation is assumed to be 20% of the mean value. |
| Self-consumption (%/year) | 20 | 10 | The mean value is assumed. The standard deviation is assumed to be 50% of the mean value. |
| Discount rate (%) | 1.4 | 0.28 | The mean value is from Lindahl et al. (2022). The standard deviation is assumed to be 20% of the mean value. |
| Crop profit (€/ha/year) | 133 | 26.6 | The standard deviation is assumed to be 20% of the mean value. |
| Crop yield/profit reduction due to shadings (%) | 25 | 5 | The standard deviation is assumed to be 20% of the mean value. |

constituting a ~45% and ~49% decrease, respectively.

For the crop yield analysis, the focus is on the total dry matter (DM) yield per hectare. The yield for the individual cuts varies depending on the yearly variation in temperature, precipitation, and other local climatic factors. Therefore, the total yearly crop yield is a better parameter

**Table 7**
Precipitation (mm) for the period May–August 2021 and 2022 compared to the reference period 1990–2010 (SMHI, 2023).

| Month | 2021 | 2022 | Reference period 1990–2010 |
|---|---|---|---|
| May | 119 | 60 | 44 |
| June | 43 | 38 | 69 |
| July | 89 | 39 | 77 |
| August | 109 | 99 | 71 |

to analyse since there is less variation between years. The crop yield results per cut are provided in the Appendix. Given the crop samples in Figs. 5 and 6, it must be noted that it is only possible to directly compare values for 2021 against 2022 for groups D and E, given the increased number of sampling plots in 2022 for groups A, B, C, and R. The total crop yield results from the samples for 2021 and 2022 are presented in Table 8. It must be noted that the actual crop yield of the field in kg DM/ha should consider the losses due to the unused land. Those losses for the APV system are about 10%, as described by Campana et al. (2021), if no specific agricultural management practices are applied (i.e., adopting special agricultural machinery to harvest the grass underneath the PV modules' supporting structure or animal grazing). The losses due to unused land in the CGMPV system are about 45%, as calculated in Table 5.

The crop yield in 2021 was higher compared to 2022 but showed a wider variation between the groups. The statistical analyses showed a significant difference in total crop yield between group R and group D in 2021. For 2022, statistical analyses showed no significant differences between the groups. Similar results were achieved in Kannenberg et al. (2023), who showed that, although light availability in a managed semi-arid grassland in Colorado, USA was reduced by 38%, the above-ground net primary productivity was reduced by only 6–7%. Similar results were also reported in Sturchio et al. (2024), where no statistical difference was observed comparing the productivity of grassland under the APV system without grazing and grassland in the control area.

The weather conditions might explain the higher yield in 2021, with abundant rain in May, which gives good conditions even for an average or dry June and July. Another factor is that the third cut in 2021 was performed later than in 2022, giving more growth time. A further factor affecting the variation across the groups could have been the lack of nutrients in 2021, since adding fertilizer in 2022 reduces this variation.

One of the limitations of this study is connected to the wide variety of species across groups, as shown in the botanical analyses presented in Fig. 7. The differences in botanical composition among the groups make analysing the single effect of shading on crop production more challenging. Nevertheless, installing an APV system on an established ley grass field represents a likely actual situation in the APV sector in Sweden and, thus, a case worth investigating. After two years of experiments on an established ley grass field, in spring 2023, our research group started investigating a typical Swedish crop rotation.

From a LER perspective, as calculated by Dupraz et al. (2011), assuming the simulated electricity production, the net area provided in Table 5, and the average crop yield in Table 8, the APV system showed an LER of 1.27 in 2021 and 1.39 in 2022. The LER values justify implementing the APV system from a land-use efficiency perspective. A summary of the LER calculation is provided in Table 9.

**Table 8**
Total DM yield in 2021 and 2022 and statistical analyses for the crop yield using Tukey Pairwise Comparisons (see Figs. 5 and 6 for the position of the groups).

| Area | 2021 | | | 2022 | | |
|---|---|---|---|---|---|---|
| | Number of samples | Mean kg DM/ha | Grouping[a] | Number of samples | Mean kg DM/ha | Grouping[a] |
| Group A | 5 | 6348 | ab | 10 | 5044 | a |
| Group B | 5 | 6660 | ab | 10 | 5454 | a |
| Group C | 5 | 6265 | ab | 10 | 4634 | a |
| Group D | 5 | 4746 | b | 5 | 5444 | a |
| Group E | 5 | 6119 | ab | 5 | 5668 | a |
| Group R | 5 | 7894 | a | 10 | 5326 | a |

[a] Grouping information using the Tukey Method and 95% confidence. Means that do not share a letter are significantly different.

#### 4.1.2. Crop metabolized energy content

The metabolized energy content analyses show typical values for ley grass (Spörndly, 2003) as summarized in Table 10, and there is a slight variation within the groups of about ±1–2%. A higher value indicates a crop with more carbohydrates produced in photosynthesis.

As in the study of the total yield, group R is used as a reference for the energy content. Few samples are significantly different using the Tukey *post-hoc* method. Studying the six cuts, groups A, C, D, and E are statistically different from group R in few comparisons. When just studying the values in Table 10, it is notable that 21 out of 30 samples' mean values for groups A–E show higher metabolized energy contents than group R.

#### 4.1.3. Crop crude protein

The analyses of the crude protein show average, typical values for ley grass (Spörndly, 2003), but there is a significant variation between the plots, especially in the third cut, as provided in Table 11. A high value is an indicator that plants have enough nutrients.

As for energy, the influence of the PV modules is studied using group R as a reference. Using the Tukey *post-hoc* method, more differences are found for the crude protein. Studying the six cuts, groups A, C, and D are statistically different from group R in at least three cuts, and Group B is different from Group R in one cut. When just studying the values in Table 11, it is notable that 25 out of 30 samples show higher samples' mean values for crude protein than group R. The available nitrogen is a significant factor in the high crude protein content. If there is high legume content, it also adds more protein to the sample. Another factor is the total yield, where a high yield can reduce protein content.

**Table 9**
LER calculations.

| Contribution of PV electricity production to LER | | | | |
|---|---|---|---|---|
| | Electricity production (kWh/kW$_p$/1$^{st}$ year) | Installed capacity (kW$_p$) | Net area (m$^2$) | Specific production per net area (kWh/m$^2$/1$^{st}$ year) |
| **CGMPV** | 1116 | 11.8 | 157 | 84 |
| **APV** | 1067 | 22.8 | 537 | 45 |
| **Contribution of PV to LER** | 0.54 | | | |
| **Contribution of crop production to LER** | | | | |
| | **Average yield in 2021 (kg DM/ha)** | | **Average yield in 2022 (kg DM/ha)** | |
| **APV** | 5782[a] | | 4540[a] | |
| **Reference area** | 7894 | | 5326 | |
| **Contribution of crop production to LER** | 0.73 | | 0.85 | |
| **LER** | | | | |
| **Year** | 2021 | | 2022 | |
| **LER** | 1.27 | | 1.39 | |

[a] Value reduced by 10% due to land loss for the supporting structure of the PV modules.

**Table 10**
Statistical analyses for the metabolized energy (MJ/kg DM) for first, second, and third cut in 2021 and 2022 using Tukey Pairwise Comparisons. Values in bold refer to mean values for the groups A–E higher than group R.

| Area | Number of samples | Metabolized energy 2021 | | Number of samples | Metabolized energy 2022 | |
|---|---|---|---|---|---|---|
| | | Mean MJ/kg DN | Grouping[a] | | Mean MJ/kg DM | Grouping[a] |
| **First cut** | | | | | | |
| Group A | 5 | **10.79** | a | 10 | **10.47** | c |
| Group B | 5 | **10.78** | a | 10 | **10.53** | bc |
| Group C | 5 | **10.69** | ab | 10 | **10.72** | ab |
| Group D | 5 | **10.52** | ab | 5 | **10.95** | a |
| Group E | 5 | **10.53** | ab | 5 | **10.62** | bc |
| Group R | 5 | 10.38 | b | 10 | 10.44 | c |
| **Second cut** | | | | | | |
| Group A | 5 | 8.97 | bc | 10 | **10.22** | ab |
| Group B | 5 | **9.73** | a | 10 | **10.58** | a |
| Group C | 5 | 9.24 | abc | 10 | **10.30** | ab |
| Group D | 5 | 9.00 | bc | 5 | 9.98 | b |
| Group E | 5 | 8.68 | c | 5 | 9.87 | b |
| Group R | 5 | 9.48 | ab | 10 | 10.17 | b |
| **Third cut** | | | | | | |
| Group A | 5 | **10.70** | ab | 10 | **10.25** | ab |
| Group B | 5 | **10.66** | ab | 10 | 10.15 | b |
| Group C | 5 | **10.79** | a | 10 | **10.42** | ab |
| Group D | 5 | **10.73** | ab | 5 | **10.68** | a |
| Group E | 5 | 10.38 | b | 5 | 10.16 | ab |
| Group R | 5 | 10.48 | ab | 10 | 10.22 | ab |

[a] Grouping information using the Tukey Method and 95% confidence. Means that do not share a letter are significantly different.

**Table 11**
Statistical analyses for the crude protein (g/kg DM) for the first, second, and third cut in 2021 and 2022 using Tukey Pairwise Comparisons. Values in bold refer to mean values for the groups A–E higher than group R.

| Area | Number of samples | Crude protein 2021 | | Number of samples | Crude protein 2022 | |
|---|---|---|---|---|---|---|
| | | Mean g/kg DM | Grouping[a] | | Mean g/kg DM | Grouping[a] |
| **First cut** | | | | | | |
| Group A | 5 | **129.1** | ab | 10 | **122.0** | a |
| Group B | 5 | **125.6** | ab | 10 | **101.5** | b |
| Group C | 5 | **142.8** | a | 10 | **124.9** | a |
| Group D | 5 | **131.6** | ab | 5 | **137.9** | a |
| Group E | 5 | 94.8 | c | 5 | 75.6 | c |
| Group R | 5 | 118.3 | b | 10 | 82.6 | c |
| **Second cut** | | | | | | |
| Group A | 5 | **107.0** | bc | 10 | **107.1** | ab |
| Group B | 5 | **115.5** | abc | 10 | **94.9** | bc |
| Group C | 5 | **118.6** | ab | 10 | **114.4** | a |
| Group D | 5 | **134.0** | a | 5 | **115.9** | a |
| Group E | 5 | 93.4 | c | 5 | 88.6 | c |
| Group R | 5 | 105.6 | bc | 10 | 94.4 | bc |
| **Third cut** | | | | | | |
| Group A | 5 | **178.1** | a | 10 | **130.1** | a |
| Group B | 5 | **150.2** | bc | 10 | **120.9** | ab |
| Group C | 5 | **167.7** | ab | 10 | **131.3** | a |
| Group D | 5 | **171.5** | ab | 5 | **135.4** | a |
| Group E | 5 | 132.0 | c | 5 | **110.0** | b |
| Group R | 5 | 139.4 | c | 10 | 109.7 | b |

[a] Grouping information using the Tukey Method and 95% confidence. Means that do not share a letter are significantly different.

Group E shows a lower content in most of the samples. Looking at the botanic composition in Fig. 7, it is not evident that this can be the explanation. Nevertheless, since the crop was not divided into species, it is not easy to draw detailed conclusions.

### 4.2. Soil moisture

The soil moisture data measured in 2022 are depicted in Fig. 8. The measurements are plotted as a scatter plot due to the lack of a complete time series during the agricultural season. The soil moisture sensors at 10 cm depth installed in the centre of the APV system rows showed higher soil moisture values than the reference ground control plot. Higher soil moisture values were measured from the soil moisture sensors in group C that were close to the PV modules and subjected to higher shading than those in group B. Interestingly, for the measurements performed at 20 cm depth, lower soil moisture values were recorded in groups B and C as compared to group R at the beginning of the measurement campaign in May 2022. Nevertheless, higher soil moisture values were measured in groups B and C compared to group R towards the end of August 2022. This seasonal trend might be explained (but it still needs to be verified) in terms of the APV system having acted as a barrier for snow, leading to lower snow depth values within the APV rows than in the reference open-field area and, thus, lower snow water equivalent. As shown in previous studies, such as by Hassanpour Adeh et al. (2018), Amaducci et al. (2018), and Wu et al. (2022), the shading produced by APV systems leads to higher soil moisture values and thus to preferable conditions for biomass growth. The soil moisture measurements campaign did not extensively cover different points and depths of the APV system and reference ground, and we cannot therefore accurately explain whether the higher soil moisture under the APV system positively affected crop yield and quality.

### 4.3. Leaf area index

The results concerning the LAI are presented in Figs. 9 and 10. The LAI measurements for groups A–C were carried out on June 23, 2022, July 5, 14, and 28, and August 12 and 25, with five replicates for each measurement. Fig. 9 shows the average trend of the LAI measurements in group R compared to the average LAI measurements under the APV system (i.e., groups A–C). On average, the LAI is 12% higher under the APV field than group R, with a peak of 24.2%. In Fig. 10, the measurements under the APV system are split between group B in the middle of the APV field and groups A and C on the edges of the APV field. On

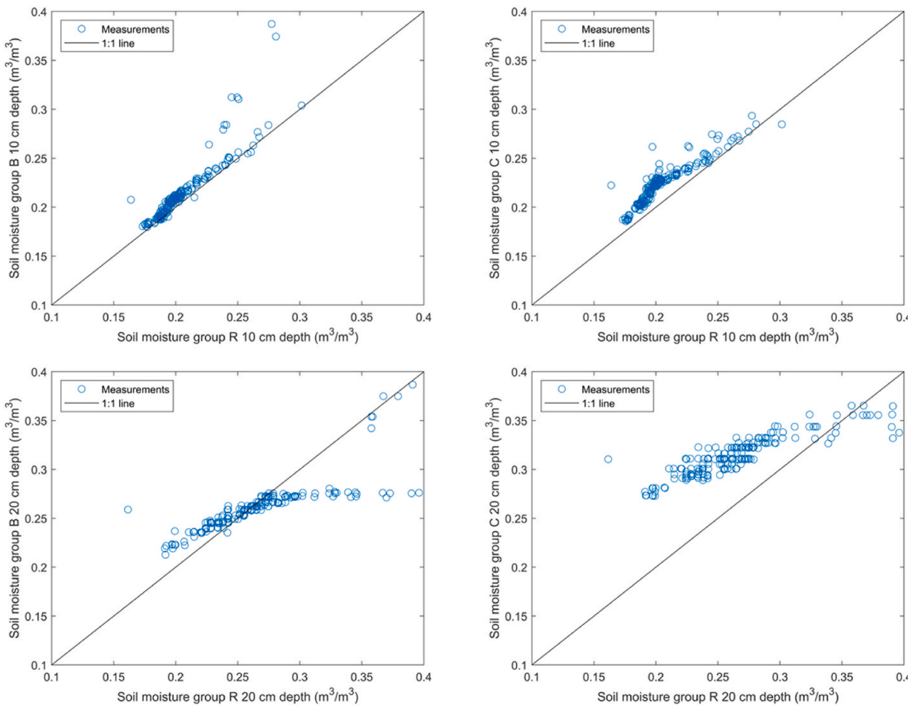

**Fig. 8.** Soil moisture ($m^3/m^3$) data comparison between group R and groups B and C at 10 cm and 20 cm depths in 2022.

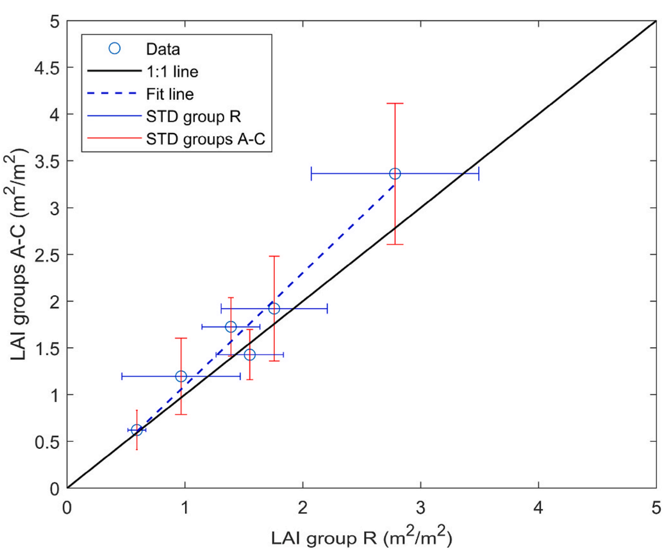

**Fig. 9.** Comparison of Leaf Area Index (LAI) ($m^2/m^2$) measurements between group R and groups A–C in 2022.

average, the LAI values in groups A–C show higher values than group R. In Fig. 10, the measurements under the APV system that show a statical difference with group R are highlighted. The statistical analyses were performed as one-way ANOVA. Four out of six measurements in group B and in groups A–C are statistically different compared to group R. The mechanism of increasing LAI under shading conditions is a common adaptation measure investigated in several studies, such as in Marrou et al. (2013) for lettuce, in Weselek et al. (2021) for winter wheat, potatoes, and grass-clover, and in Potenza et al. (2022) for soybean, with similar conclusions. Despite a PAR reduction between the APV system of about 25% (Campana et al., 2021; Campana et al., 2022a; Zainali et al., 2023b), no statistically significant difference was observed between the yield of the samples under the APV system compared to the yield of the samples in group R, as shown in Table 8. These results can be partially explained by the LAI increase and an enhanced radiation use efficiency under the APV system due to a higher fraction of diffuse PAR. The higher fraction of diffuse PAR compared to group R is due to the complex shading conditions under which the crop grows beneath the APV system. As reviewed by Ma Lu et al. (2022), a high fraction of diffuse PAR is closely correlated with higher light-use efficiency and increased $CO_2$ assimilation, and thus more efficient photosynthesis.

### 4.4. Crop modelling validation

The crop model calibration and validation results are presented in Fig. 11 for the reference area. In particular, the crop yield at different cuts and the total crop yield are reported for the following: a) average measured crop yield in group R, b), simulated crop yield with literature values provided in Table 3, c) simulated crop yield after calibration, and d) simulated crop yield after an advanced calibration using two biomass–energy ratios for the first two cuts and last cut separately. From Fig. 11, the use of literature data for crop modelling leads to accurate seasonal crop yield assessment (i.e., ~3% percentage accuracy). However, the crop yield estimation across the different cuts shows significant differences from the actual measurements. The model calibration shows that there is a percentage accuracy of ~9% from the actual measurements on a seasonal basis, with the model tending to overestimate the seasonal crop yield. After model calibration, the modelling results show that the model can produce crop yield results that follow the actual trend of the measured crop yield across the three cuts. The best-performing results are achieved using two different biomass–energy ratios, as highlighted in Schils et al. (2013), with high accuracy both on the single cuts and on the seasonal crop yield.

The crop modelling results under the APV system for 2022 are summarized in Fig. 12. The results show the comparison between the average yield under the APV system with the average yield simulated by Agri-OptiCE®. The calibrated model in Fig. 12 refers to the model calibrated with two biomass–energy ratios, as performed in Fig. 11, while Agri-OptiCE® calibrated advanced adaptation refers to the model calibrated in Fig. 11 with a maximum LAI increase of 12% as measured in Section 4.3. From Fig. 12, two main conclusions can be drawn. The

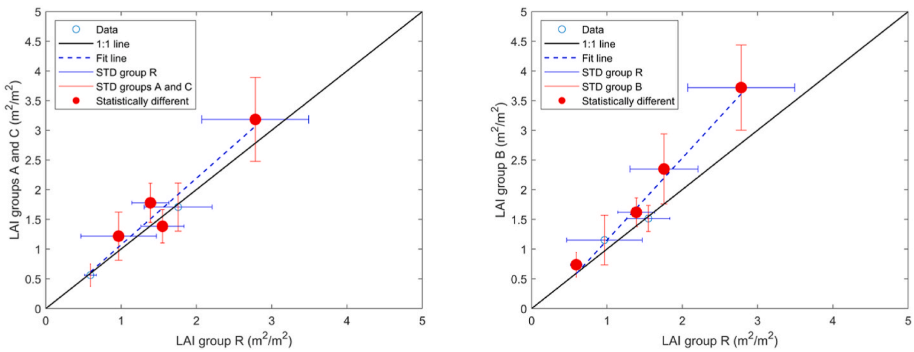


**Fig. 10.** Comparison of Leaf Area Index (LAI) (m$^2$/m$^2$) measurements between group R and groups A and C (left), and between group R and group B (right) in 2022.

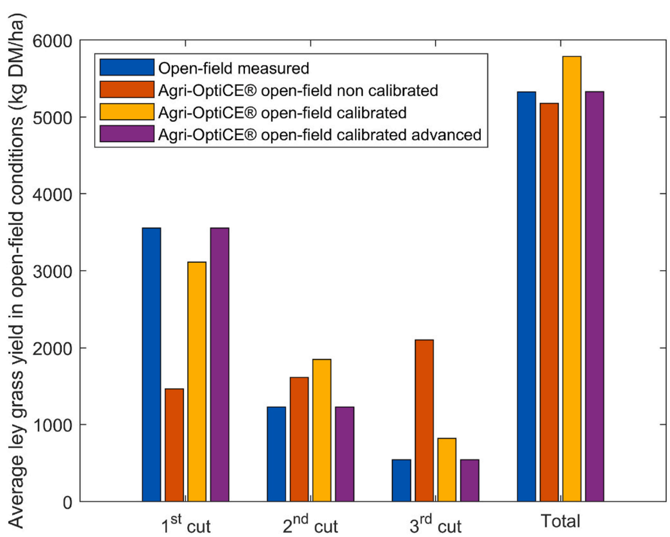


**Fig. 11.** Average ley grass yield (kg DM/ha) in 2022 in open-field conditions versus simulated yield using the integrated modelling platform Agri-OptiCE®.

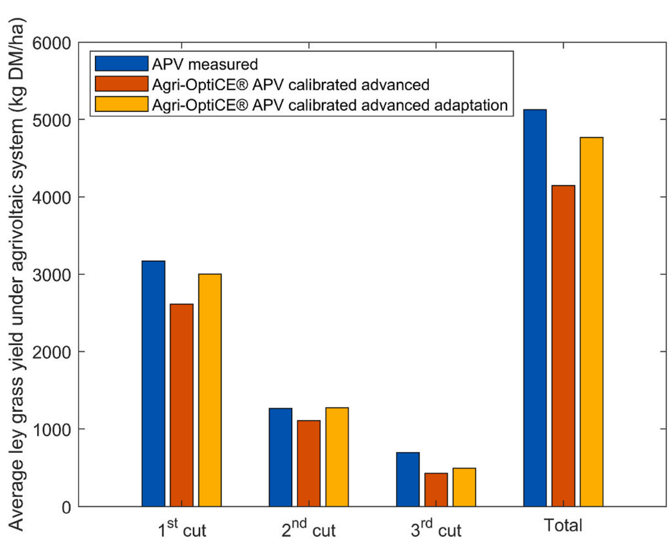


**Fig. 12.** Average ley grass yield (kg DM/ha) in 2022 under the APV system versus simulated yield using the integrated modelling platform Agri-OptiCE®.

first conclusion is that the calibrated model shows a percentage accuracy of ~19% compared to the actual measurements of the average crop yield under the APV system, and, given the complexities of the modelling, it can still be considered a good result. Potenza et al. (2022) applied the model developed by Amaducci et al. (2018) to simulate the effects of shading on the grain yield of soybean. They reported different normalized root mean square errors between predicted and observed yields ranging between 12.9% and 2.82% depending on different shading levels. They observed that the integrated modelling platform tended to underestimate the crop yield while the shading level increased.

As highlighted in Campana et al. (2021), the developed modelling platform can simulate the worst-case scenario for the impact of shadings on crop yield if no crop adaptation measures are quantified or available. Such modelling and results can be of extreme importance while predicting crop yields under APV systems for assessing the performance of future installations – for instance, at the design and permit stages. The second conclusion is that, as highlighted in Campana et al. (2021), the model's accuracy can be enhanced by supplying the model with adjusted input parameters that can further depict the adaptation measures of crops under shading conditions. Compared to the measured results, the model developed in this study underestimates the crop yield under shading conditions by 7% compared to the actual average measured values, when adaptation measures are fed into the model. This result shows how important the availability of crop adaptation measures is for accurately estimating crop yield under shading conditions. As pointed out in Section 1, the crop yield under APV systems and its percentage reduction compared to open-field conditions is one of the most crucial key performance indicators for APV systems; they are targets or design parameters in laws regulating APV systems. High accuracy crop yield in an integrated APV platform can significantly impact the design of an APV system such that it meets policy requirements and, thus, the cost-benefit analysis of the system.

### *4.5. Economic perspective*

The results of the economic analysis are partly depicted in Fig. 13 in terms of discounted cumulative cash flow for the reference CGMPV system, for the APV system combined with a traditional crop rotation, and for the APV system owned and managed by a third-party company to which the land is leased by the farmer. The discounted cumulative cash flow for the crop rotation is also provided. It is multiplied by 10 for an easier visualization. The NPVs and DPBPs for the investigated scenarios and cases are summarized in Table 12.

Concerning the crop yield reduction under shading conditions, we have assumed no reduction for the permanent ley grass, given the results in Section 4.1.1. Nevertheless, the actual crop yield under the APV system should be reduced by 10% due to the non-harvestable area close to the PV modules' supporting structures. For the crop rotation, we have assumed a reduction of about 25%, given the simulation results in Campana et al. (2021, 2022a) and Zainali et al. (2023b) concerning PAR reduction under APV systems and lack of experimental data.

The APV system shows a significantly lower NPV (i.e., the last value of the discounted cumulative cash flow diagram) than the reference CGMPV system, i.e., 46.2 k€ for the system combined with permanent

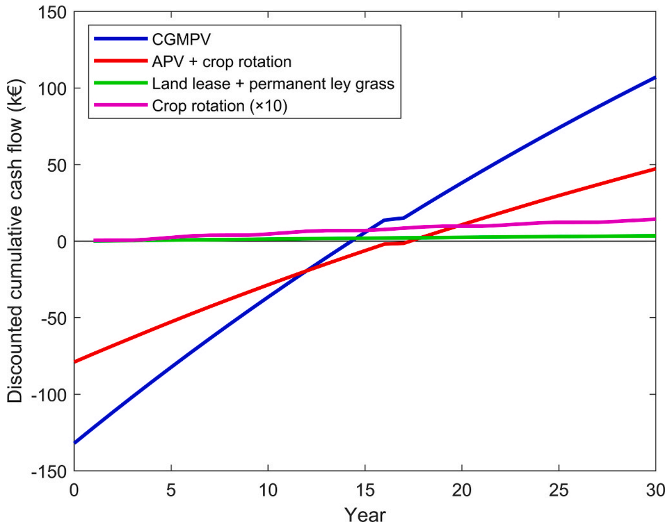


**Fig. 13.** Discounted cumulative cash flows for the reference CGMPV system, for the APV system with crop rotation, for the APV system owned and managed by a third-party company to which the land is leased by the farmer, and for the crop rotation.

**Table 12**
NPVs and DPBPs of the investigated scenarios and cases.

| Scenario/case | NPV (k€) | DPBP (years)[a] | Comment |
|---|---|---|---|
| CGMPV system owned by farmer | 107 | 14.3 | NPV considers revenue from PV electricity production only. |
| APV system owned by farmer; permanent ley grass | 46.2 | 17.4 | NPV considers revenues from PV electricity and crop production. |
| APV system owned by farmer; crop rotation | 47.2 | 17.4 | NPV considers revenues from PV electricity and crop production. |
| APV system owned by third-party company; permanent ley grass maintained by farmer | 3.5 | – | NPV considers revenues from land lease and crop production. |
| Permanent ley grass | 0.1 | – | NPV considers revenue from crop production only. |
| Crop rotation | 1.4 | – | NPV considers revenue from crop production only. |

[a] The DPBP refers only to the CGMPV or APV system investment.

ley grass compared to 107 k€, respectively. This result is mainly due to lower electricity production and higher investment costs (see Table 5). The DPBP for the CGMPV system is 14.3 years versus 17.4 years for the APV system. Although the crop rotation shows better profit than permanent ley grass, the effect on the NPV of the APV system is minimal. Moreover, it can be noted that, from a farmer's perspective, the area used for the installation of an APV system can lead to a 30-year profit of ~30 times (for the crop rotation) to more than 600 times (for the permanent ley grass) higher compared to agricultural production with EU farmer support, based on the input data in Table 5. Leasing the land while maintaining the permanent ley grass leads to a NPV of 3.5 k€, which is more than 40 times higher compared to only permanent ley grass. Those results agree with the results obtained by Cuppari et al. (2021) that showed that the co-location of PV systems and agriculture can increase the relative net annual incomes of a farm in the range between 300% and 5000% as compared to the agriculture-only scenario. The effect of the yield on the annual crop profit per hectare and consequently on the APV system profit has been investigated by performing a sensitivity analysis using the values by Rosenqvist (2019) referring to "low yield" and "high yield" as compared to those in Table 5 referring to "medium to high yield". The results of the sensitivity analysis are depicted in Table 13. The effect of the crop yield and, thus, profit for the investigated area shows a nonsignificant effect on the NPV of the APV system.

The results of the Monte Carlo Analysis for an APV system built on a 0.2 ha plot owned by the farmer in terms of distribution of the NPV are depicted in Fig. 14. At the same time, Table 14 summarizes the PCCs for the sensitive parameters listed in Table 6.

In the 500 runs of the Monte Carlo Analysis, 98% of the runs provided a positive NPV, showing a significant tendency for the project to be profitable. The most impactful parameters affecting the NPV of the project are the PV system-specific costs (PCC = −0.58), the selling electricity price (PCC = 0.57), the specific electricity production (PCC = 0.45), and the electricity buying price (PCC = 0.26). The average annual crop profit and the average crop yield/profit reduction due to shading for the crop rotation showed a nonsignificant influence on the NPV with one of the lowest PCCs.

Although APV systems represent an intelligent solution to avoid the conflict between land use for food production versus energy conversion and they increase land use efficiency, specific laws should protect crop production. Indeed, despite APV systems allowing the coexistence of food and electricity production, an analysis of the results of Fig. 13 and Tables 12–14 gives reason to suspect that the high revenues for PV electricity might discourage farmers from conducting agricultural activities, leading to situations like a CGMPV system where land is used only for PV production.

## 5. Conclusions

This study summarizes some of the most important results of establishing Sweden's first APV system – specifically, the results concerning crop yield and properties observed under the APV system as compared to open-field conditions. The crop yield results are used to calibrate and validate an integrated modelling platform for simulating and optimizing APV systems. The economic aspects of implementing APV systems in Sweden are also addressed by analysing the benefits produced as compared to CGMPV systems and agriculture-only.

The following conclusions and implications can be drawn:

- The statistical analyses of the samples showed a significant difference in total crop yield only between group R (i.e., reference area) and group D (i.e., between the rows of the CGMPV system) in 2021. For 2022, statistical analyses of the samples showed no significant differences between the groups. The actual crop yield of the field in kg DM/ha should consider the losses due to the unused land. Those losses for the vertically mounted APV system are about 10%, as described by Campana et al. (2021). Similar results concerning grassland productivity were achieved in Kannenberg et al. (2023) and in Sturchio et al. (2024) for semi-arid grassland in the USA.
- 21 out of 30 samples' mean values show metabolized energy content values higher than group R. 25 out of 30 samples' mean values show crude protein values higher than group R.

**Table 13**
Effect of crop yield and profit on the APV system profitability.

| Scenario/case | NPV (k€) |
|---|---|
| APV system owned by farmer; permanent ley grass (medium to high yield) | 46.2 |
| APV system owned by farmer; permanent ley grass (low yield) | 46.1 |
| APV system owned by farmer; permanent ley grass (high yield) | 46.4 |
| APV system owned by farmer; crop rotation (medium to high yield) | 47.2 |
| APV system owned by farmer; crop rotation (low yield) | 46.4 |
| APV system owned by farmer; crop rotation (high yield) | 47.7 |

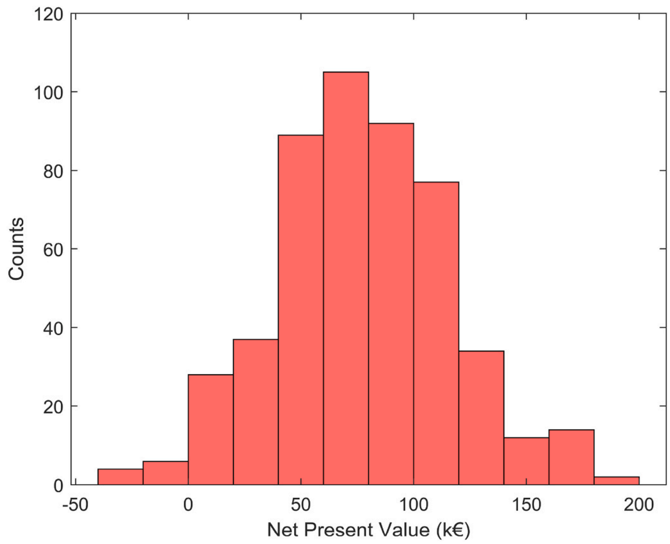


**Fig. 14.** Net Present Value distribution.

**Table 14**
Pearson Correlation Coefficients (PCCs) for the investigated sensitive parameters.

| Sensitive parameter | Pearson Correlation Coefficient |
|---|---|
| Specific electricity production (kWh/kW$_p$/1$^{st}$ year) | 0.45 |
| PV system specific cost (€/kW$_p$) | −0.58 |
| Operation and maintenance (% system cost/year) | −0.14 |
| Inverter replacement (€/kW$_p$) | 0.00 |
| Electricity selling price (€/kWh) | 0.57 |
| Electricity buying price (€/kWh) | 0.26 |
| Self-consumption (%/year) | 0.10 |
| Discount rate (%) | −0.01 |
| Average crop profit (€/ha/year) | 0.04 |
| Average crop yield/profit reduction due to shading (%) | 0.01 |

- The measurements of the LAI showed a tendency to increase under shading conditions. On average, the LAI under the APV field is 12% higher than group R, with a peak of 24.2%.
- Higher soil moisture values were reported at different soil depths under the APV system compared to the reference area in the open field. Nevertheless, due to the lack of an extensive soil moisture measurement campaign across different points and depths of the APV system and reference area, we cannot accurately explain whether the higher soil moisture under the APV system affected crop yield and quality.
- The calibrated crop sub-model of the integrated modelling platform for APV systems showed a difference of 19% compared to the actual measurements of the average crop yield under the APV system. Supplying the model with adjusted input parameters that can further depict the adaptation measures of crops under shading conditions can enhance the model's accuracy. Compared to the measured results, the model developed in this study underestimates the crop yield under shading conditions by ~7% compared to the actual average measured values.
- The integrated APV modelling platform validation has significant positive implications concerning the estimation of ley grass productivity before the actual installation of an APV and thus concerning the large-scale deployment of APV systems. This is a timely issue because more countries are adopting APV policies that set crop yield targets as regulatory requirements (Dupraz, 2023). Pre-installation prediction of crop yields under APV systems will become more important for the permit process of APV projects to meet policy requirements.
- From a farmer's perspective, using an area for installing an APV system can lead to a 30-year profit of ~30 times (for the investigated crop rotation) up to more than 600 times (for permanent ley grass) that of agricultural production alone, even considering EU farmer support.
- At parity of total ground area, the APV system shows a significantly lower NPV than the reference CGMPV system, i.e., 46.2 k€ for APV system combined with permanent ley grass compared to 107 k€.
- The Monte Carlo Analysis for a 0.2-ha APV system serving a farm showed that 98% of the runs provided a positive NPV, showing a significant tendency for the project to be profitable. The parameters that most strongly affects the NPV of the project are the PV system specific investment costs, the electricity selling price, the specific electricity production, and the electricity buying price.
- Elkadeem et al. (2023) reported that the potential of pasture areas in Sweden in terms of implementing APV systems is ~87 GW$_p$, corresponding to ~80 TW h/year, which constitutes ~56% of the total electricity consumption in 2021 (Statistics Sweden, 2023). The results of this study concerning the crop yield, metabolized energy content, crude protein, and economy showed that the implementation of APV systems on ley grass areas and potentially on pastures can be a win–win solution for the energy and forage sectors, while also supporting farmers economies.

## CRediT authorship contribution statement

**Pietro Elia Campana:** Conceptualization, Methodology, Software, Validation, Formal analysis, Investigation, Data Curation, Writing – original draft, Writing – review & editing, Project administration, Funding acquisition. **Bengt Stridh:** Conceptualization, Formal analysis, Investigation, Writing – original draft, Writing – review & editing. **Torsten Hörndahl:** Conceptualization, Methodology, Validation, Formal analysis, Investigation, Data Curation, Writing – original draft, Writing – review & editing. **Sven-Erik Svensson:** Conceptualization, Methodology, Validation, Formal analysis, Investigation, Data Curation, Writing – original draft, Writing – review & editing. **Sebastian Zainali:** Validation, Formal analysis, Investigation, Data Curation, Writing – original draft, Writing – review & editing. **Silvia Ma Lu:** Validation, Formal analysis, Investigation, Data Curation, Writing – original draft, Writing – review & editing. **Tekai Eddine Khalil Zidane:** Writing – original draft, Writing – review & editing. **Paolo De Luca:** Validation, Formal analysis, Investigation, Data Curation, Writing – original draft, Writing – review & editing. **Stefano Amaducci:** Formal analysis, Investigation, Data Curation, Writing – original draft, Writing – review & editing. **Michele Colauzzi:** Formal analysis, Investigation, Data Curation, Writing – original draft, Writing – review & editing.

## Declaration of competing interest

The authors declare the following financial interests/personal relationships which may be considered as potential competing interests: The company European Energy Sverige AB is financing half of Sebastian Zainali's Ph.D. salary.

## Data availability

Data will be made available on request.

## Acknowledgements

The authors acknowledge the financial support received from the Swedish Energy Agency through the project "Evaluation of the first agrivoltaic system in Sweden", grant number 51000–1, that allowed the establishment of the first experimental agrivoltaic system in Sweden at

Kärrbo Prästgård. The authors also aknowledge the support received from Dr Jan-Eric Englund at SLU Alnarp on the statistical analyses. The first author acknowledges Formas for the funding received through the early career project “Avoiding conflicts between the sustainable development goals through agro-photovoltaic systems”, grant number FR-2021/0005. The authors also acknowledge the funding received from the Swedish Energy Agency through the project “SOLVE”, grant number 52693–1. Furthermore, the authors acknowledge the Future Energy Centre at Mälardalen University for the internal projects “World-class agrivoltaic system” and “Enhancing the scientific relevance and safety of the first agrivoltaic system in Sweden”, which have significantly improved the solar irradiance and microclimate monitoring of the experimental agrivoltaic system. The author Paolo De Luca received funding from the European Union’s Horizon Europe Research and Innovation Programme under grant agreement No. 101059659.

## Appendix

The chemical characteristics of the soil measured in 2021 and summarized in Table A1 show normal values for soil with high clay content which has been in pasture for a long time. The only notable point is that assimilable phosphorus in sample group C is much lower than the other groups.

**Table A1**
Soil characteristics measured in 2021

| Samples ID/group | 1–5/A | 6–10/B | 11–15/C | 26–30/R |
|---|---|---|---|---|
| pH | 5.8 | 6.0 | 6.0 | 5.9 |
| **Assimilable P** (mg/100g) | 6.3 | 12.2 | 3.7 | 8.1 |
| **Assimilable K** (mg/100g) | 24.2 | 32.4 | 21.0 | 27.3 |
| **Assimilable Mg** (mg/100g) | 45.1 | 49.6 | 40.4 | 46.1 |
| **K/Mg-AL** | 0.5 | 0.7 | 0.5 | 0.6 |
| **Assimilable Ca** (mg/100g) | 274 | 359 | 237 | 258 |
| **Assimilable Al** (mg/100g) | 27 | 26 | 28 | 25 |
| **Assimilable Fe** (mg/100g) | 45 | 45 | 47 | 37 |
| **K–HCl** (mg/100g) | – | – | – | – |
| **P–HCl** (mg/100g) | – | – | – | – |
| **Cu–HCl** (mg/100g) | – | – | – | – |
| **B** (mg/kg) | – | – | – | – |
| **Organic matter** (%) | 6.0 | 7.1 | 5.9 | 6.6 |
| **Clay** (%) | 31 | 31 | 31 | 30 |
| Loam (%) | 49 | 48 | 48 | 48 |
| **Sand** (%) | 14 | 14 | 15 | 15 |
| **Classification** | loamy soil intermediate clay | loamy soil intermediate clay | moderately humus-rich intermediate clay | loamy soil intermediate clay |
| **C-tot** (g/kg) | 35 | 40 | 34 | 38 |
| **N-tot** (g/kg) | 3.2 | 3.6 | 3.1 | 3.4 |
| **Ca-tot** (g/kg) | 5.4 | 6.6 | 5.5 | 5.7 |

The crop yield results per cuts and year are depicted in Figures A1–A6.

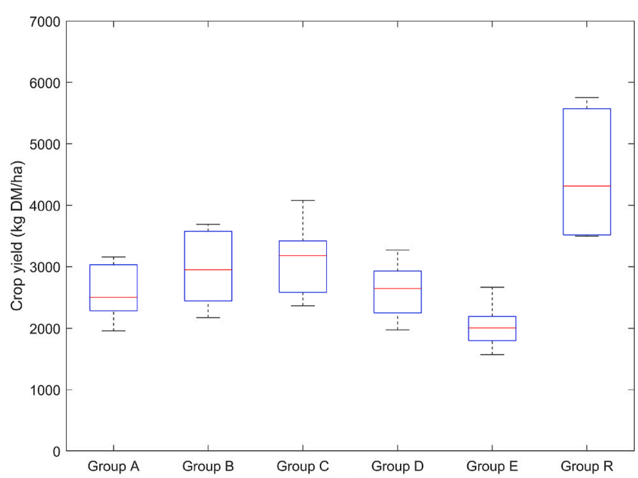


**Fig. A1.** Crop yield results for the first cut in 2021.

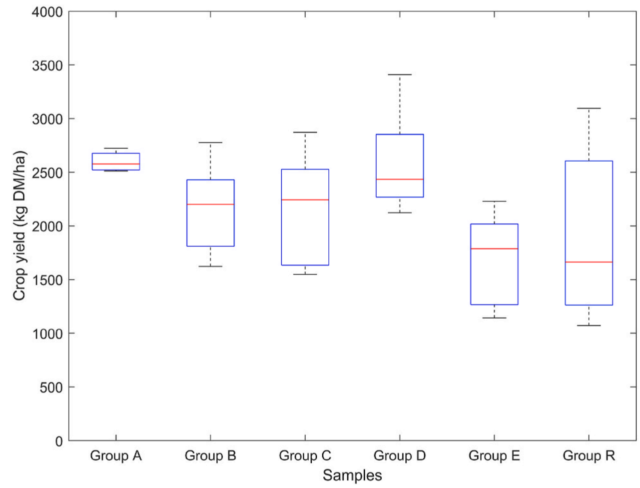


**Fig. A2.** Crop yield results for the second cut in 2021.

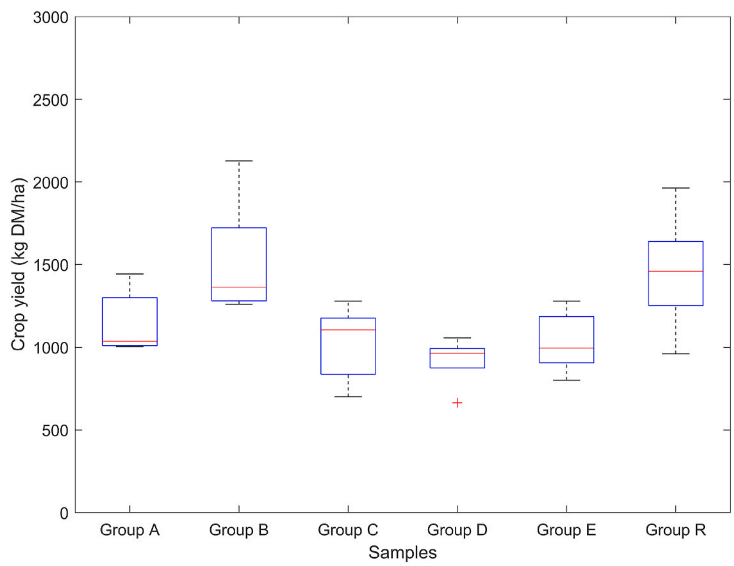


**Fig. A3.** Crop yield results for the third cut in 2021.

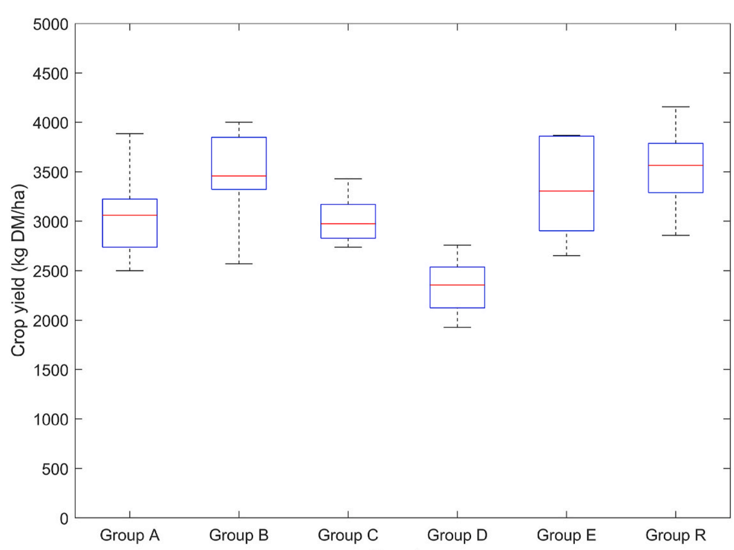


**Fig. A4.** Crop yield results for the first cut in 2022.

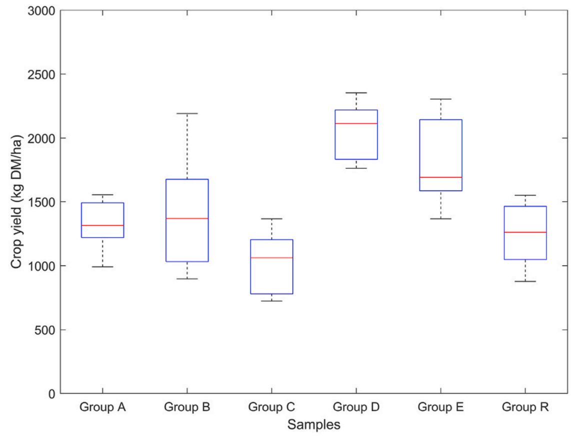


**Fig. A5.** Crop yield results for the second cut in 2022.

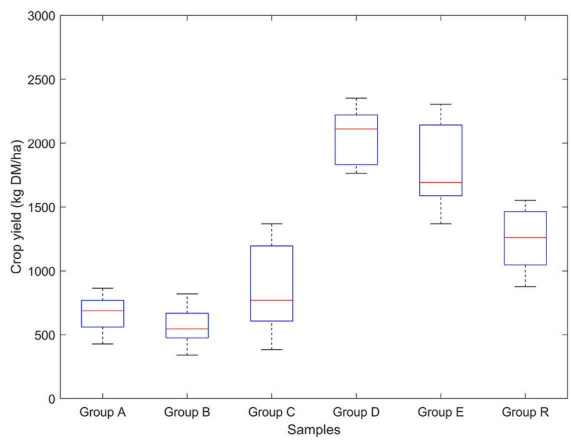


**Fig. A6.** Crop yield results for the third cut in 2022.

## References


Agostini, A., Colauzzi, M., Amaducci, S., 2021. Innovative agrivoltaic systems to produce sustainable energy: an economic and environmental assessment. Appl. Energy 281, 116102.

Åkerlind, M., Weisbjerg, M., Eriksson, T., Thøgersen, R., Udén, P., Olafsson, B.L., Harstad, O.M., Volden, H., 2011. Feed analyses and digestion methods. In: Volden, H. (Ed.), NorFor – the Nordic Feed Evaluation System. Wageningen Academic Publishers, Wageningen, The Netherlands, pp. 41–54. EAAP publication No. 130.

Al Mamun, M.A., Dargusch, P., Wadley, D., Zulkarnain, N.A., Aziz, A.A., 2022. A review of research on agrivoltaic systems. Renew. Sustain. Energy Rev. 161, 112351.

AL-agele, H.A., Proctor, K., Murthy, G., Higgins, C., 2021. A case study of tomato (Solanum lycopersicon var. legend) production and water productivity in agrivoltaic systems. Sustainability 13 (5), 2850.

Allen, R.G., Pereira, L.S., Raes, D., Smith, M., 1998. Crop evapotranspiration-Guidelines for computing crop water requirements-FAO Irrigation and drainage paper 56. FAO, Rome 300 (9), D05109.

Amaducci, S., Yin, X., Colauzzi, M., 2018. Agrivoltaic systems to optimise land use for electric energy production. Appl. Energy 220, 545–561.

Artru, S., Lassois, L., Vancutsem, F., Reubens, B., Garré, S., 2018. Sugar beet development under dynamic shade environments in temperate conditions. Eur. J. Agron. 97, 38–47.

Barron-Gafford, G.A., Pavao-Zuckerman, M.A., Minor, R.L., Sutter, L.F., Barnett-Moreno, I., Blackett, D.T., et al., 2019. Agrivoltaics provide mutual benefits across the food–energy–water nexus in drylands. Nat. Sustain. 2 (9), 848–855.

Brisson, N., Gary, C., Justes, E., Roche, R., Mary, B., Ripoche, D., et al., 2003. An overview of the crop model STICS. Eur. J. Agron. 18 (3–4), 309–332.

Brunet, C., Savadogo, O., Baptiste, P., Bouchard, M.A., Rakotoary, J.C., Ravoninjatovo, A., et al., 2020. Impacts generated by a large-scale solar photovoltaic power plant can lead to conflicts between sustainable development goals: a review of key lessons learned in Madagascar. Sustainability 12 (18), 7471.

Campana, P.E., Lastanao, P., Zainali, S., Zhang, J., Landelius, T., Melton, F., 2022b. Towards an operational irrigation management system for Sweden with a water–food–energy nexus perspective. Agric. Water Manag. 271, 107734.

Campana, P.E., Scragg, J.S., Lu, S.M., Zainali, S., Stridh, B., Amaducci, S., Colauzzi, M., 2022a. Solar Irradiance Distribution under Vertically Mounted Agrivoltaic Systems–Model Development, Validation, and Applications for Microclimate Assessment.

Campana, P.E., Stridh, B., Amaducci, S., Colauzzi, M., 2021. Optimisation of vertically mounted agrivoltaic systems. J. Clean. Prod. 325, 129091.

Campana, P.E., Zhang, J., Yao, T., Andersson, S., Landelius, T., Melton, F., Yan, J., 2018. Managing agricultural drought in Sweden using a novel spatially-explicit model from the perspective of water-food-energy nexus. J. Clean. Prod. 197, 1382–1393.

Campana, P.E., Zhang, Y., Lundblad, A., Yan, J., 2017. An open-source platform for simulation and optimization of clean energy technologies. Energy Proc. 105, 946–952.

Capellán-Pérez, I., De Castro, C., Arto, I., 2017. Assessing vulnerabilities and limits in the transition to renewable energies: land requirements under 100% solar energy scenarios. Renew. Sustain. Energy Rev. 77, 760–782.

Cascone, Y., Corrado, V., Serra, V., 2011. Calculation procedure of the shading factor under complex boundary conditions. Sol. Energy 85 (10), 2524–2539.

CropSAT, 2023. https://cropsat.com. (Accessed 16 July 2023).

Cuppari, R.I., Higgins, C.W., Characklis, G.W., 2021. Agrivoltaics and weather risk: a diversification strategy for landowners. Appl. Energy 291, 116809.

Dagens Industry, 2021. Därför är det smart att arrendera ut din mark till storskalig solenergi. Available at: https://www.di.se/brandstudio/energiengagemang/darfor-ar-det-smart-att-arrendera-ut-din-mark-till-storskalig-solenergi/. (Accessed 15 July 2023).

Deb, K., Agrawal, S., Pratap, A., Meyarivan, T., 2000. A fast elitist non-dominated sorting genetic algorithm for multi-objective optimization: NSGA-II. In: Parallel Problem Solving from Nature PPSN VI: 6th International Conference Paris, France, September 18–20, 2000 Proceedings 6. Springer Berlin Heidelberg, pp. 849–858.

Dietz, K.J., Zörb, C., Geilfus, C.M., 2021. Drought and crop yield. Plant Biol. 23 (6), 881–893.

Dinesh, H., Pearce, J.M., 2016. The potential of agrivoltaic systems. Renew. Sustain. Energy Rev. 54, 299–308.

Duffie, J.A., Beckman, W.A., 2013. Solar Engineering of Thermal Processes. John Wiley & Sons.

Dupraz, C., 2023. Assessment of the ground coverage ratio of agrivoltaic systems as a proxy for potential crop productivity. Agroforestry Systems 1–18.

Dupraz, C., Marrou, H., Talbot, G., Dufour, L., Nogier, A., Ferard, Y., 2011. Combining solar photovoltaic panels and food crops for optimising land use: towards new agrivoltaic schemes. Renew. Energy 36 (10), 2725–2732.
Elamri, Y., Cheviron, B., Lopez, J.M., Dejean, C., Belaud, G., 2018. Water budget and crop modelling for agrivoltaic systems: application to irrigated lettuces. Agric. Water Manag. 208, 440–453.
Elkadeem, M.R., Zainali, S., Lu, S.M., Younes, A., Abido, M.A., Amaducci, S., et al., 2023. Agrivoltaic systems potentials in Sweden: a geospatial-assisted multi-criteria analysis. Appl. Energy 356, 122108. Engineers, Planers and Education (2018). URL. http://www.meteonorm.com.
European Standards, 2023. DIN SPEC 9143. Agri-photovoltaic systems - requirements for primary agricultural use. Available at: https://www.en-standard.eu/din-spec-91434-agri-photovoltaic-systems-requirements-for-primary-agricultural-use/. (Accessed 18 June 2023).
Exchange Rates UK. (2023). https://www.exchangerates.org.uk/SEK-EUR-spot-exchange-rates-history-2022.html#:~:text=This%20is/20the/20Swedish/20Krona, EUR/20on/2024/20Dec/202022. Accessed 9th July 2023.
Fraunhofer ISE, 2023. Harvesting the Sun for power and produce – Agrophotovoltaics increases the land Use efficiency by over 60 percent. Available at: https://www.ise.fraunhofer.de/en/press-media/press-releases/2017/harvesting-the-sun-for-power-and-produce-agrophotovoltaics-increases-the-land-use-efficiency-by-over-60-percent.html. (Accessed 6 December 2023).
Gonocruz, R.A., Nakamura, R., Yoshino, K., Homma, M., Doi, T., Yoshida, Y., Tani, A., 2021. Analysis of the rice yield under an Agrivoltaic system: a case study in Japan. Environments 8 (7), 65.
Gonocruz, R.A., Uchiyama, S., Yoshida, Y., 2022. Modeling of large-scale integration of agrivoltaic systems: impact on the Japanese power grid. J. Clean. Prod. 363, 132545.
Gorjian, S., Campana, P.E., 2022. Solar Energy Advancements in Agriculture and Food Production Systems.
Hassanpour Adeh, E., Selker, J.S., Higgins, C.W., 2018. Remarkable agrivoltaic influence on soil moisture, micrometeorology and water-use efficiency. PLoS One 13 (11), e0203256.
Italian Ministry of the Environment and Energy Security, 2023. Guidelines in the field of Agrivoltaic systems. Available at: https://www.mase.gov.it/sites/default/files/archivio/allegati/PNRR/linee_guida_impianti_agrivoltaici.pdf. (Accessed 22 April 2023) (In Italian).
Kannenberg, S.A., Sturchio, M.A., Venturas, M.D., Knapp, A.K., 2023. Grassland carbon-water cycling is minimally impacted by a photovoltaic array. Communications Earth & Environment 4 (1), 238.
Katsikogiannis, O.A., Ziar, H., Isabella, O., 2022. Integration of bifacial photovoltaics in agrivoltaic systems: a synergistic design approach. Appl. Energy 309, 118475.
Khan, M.R., Hanna, A., Sun, X., Alam, M.A., 2017. Vertical bifacial solar farms: physics, design, and global optimization. Appl. Energy 206, 240–248.
Kiniry, J.R., Williams, J.R., Major, D.J., Izaurralde, R.C., Gassman, P.W., Morrison, M., et al., 1995. EPIC model parameters for cereal, oilseed, and forage crops in the northern Great Plains region. Can. J. Plant Sci. 75 (3), 679–688.
Laub, M., Pataczek, L., Feuerbacher, A., Zikeli, S., Högy, P., 2021. Contrasting yield responses at varying levels of shade suggest different suitability of crops for dual land-use systems. A meta-analysis. agriRxiv, 20210479141, 2021.
Li, X., Chen, W., Li, Y., 2012. Study on photosynthetic characteristics of blueberry in greenhouse. Acta Hortic. 926, 315–320.
Lindahl, J., Berard, J., Oller Westerberg, A., 2022. National survey report of PV power applications in Sweden 2021. Available at: https://iea-pvps.org/wp-content/uploads/2022/10/National-Survey-Report-of-PV-Power-Applications-in-Sweden-2021.pdf. (Accessed 15 March 2023).
Ma Lu, S., Zainali, S., Stridh, B., Avelin, A., Amaducci, S., Colauzzi, M., Campana, P.E., 2022. Photosynthetically active radiation decomposition models for agrivoltaic systems applications. Sol. Energy 244, 536–549. https://doi.org/10.1016/j.solener.2022.05.046.
Ma Lu, S., Zainali, S., Sundström, E., Nygren, A., Stridh, B., Avelin, A., Campana, P.E., 2023. Validation of vertical bifacial agrivoltaic and other systems modelling. AgriVoltaics 2023.
Marrou, H., Wéry, J., Dufour, L., Dupraz, C., 2013. Productivity and radiation use efficiency of lettuces grown in the partial shade of photovoltaic panels. Eur. J. Agron. 44, 54–66.
Martín, N., Ruiz, J.M., 2005. Annual angular reflection losses in PV modules. Prog. Photovoltaics Res. Appl. 13 (1), 75–84.
Melo, E.G., Almeida, M.P., Zilles, R., Grimoni, J.A., 2013. Using a shading matrix to estimate the shading factor and the irradiation in a three-dimensional model of a receiving surface in an urban environment. Sol. Energy 92, 15–25.
Mengi, E., Samara, O.A., Zohdi, T.I., 2023. Crop-driven optimization of agrivoltaics using a digital-replica framework. Smart Agricultural Technology 4, 100168.
Nord Pool, 2023. https://www.nordpoolgroup.com/en/. (Accessed 25 March 2023).
Nordiskaprojekt. (2023). Available at: https://www.nordiskaprojekt.se/2022/04/28/solparken-i-svedberga-till-provning-i-hogre-instans. Accessed 25th March 2023.
OptiCE. Available at: http://optice.net/. Accessed 16th July 2023.
Potenza, E., Croci, M., Colauzzi, M., Amaducci, S., 2022. Agrivoltaic system and modelling simulation: a case study of soybean (Glycine max L.) in Italy. Horticulturae 8 (12), 1160.
Remund, J., Müller, S., Kunz, S., Huguenin-Landl, B., Studer, C., Cattin, R., 2018. Meteonorm Handbook, part II: Theory. Bern, Switzerland, Meteotest.
Riaz, M.H., Imran, H., Younas, R., Butt, N.Z., 2021. The optimization of vertical bifacial photovoltaic farms for efficient agrivoltaic systems. Sol. Energy 230, 1004–1012.
Rosenqvist, H., 2019. Kalkyler För Energigrödor 2019. Jordbruksverket. Jönköping.
Scania County Administrative Board, 2023. Farmer support. Available at: https://www.lansstyrelsen.se/skane/natur-och-landsbygd/stod-till-jordbruk-och-landsbygd/jordbrukarstod.html. (Accessed 6 July 2023) (in Swedish).
Schils, R., Velthof, G., Mucher, S., Hazeu, G., Oenema, O., de Wit, A., Smit, A., 2013. Current methods to estimate grassland production and biological fixation. Available at: https://ec.europa.eu/eurostat/documents/2393397/8259002/Grassland_2014_Task+2.pdf/42873c7f-dfdf-49ca-b2ef-7c7b5bcabfc8. (Accessed 31 March 2023).
SMHI. (2023). Available at: https://www.smhi.se/data/meteorologi/ladda-ner-meteorologiska-observationer#param=airtemperatureInstant,stations=core. Accessed 19th June 2023.
Söderström, M., Piikki, K., Stenberg, M., Stadig, H., Martinsson, J., 2017. Predicting nitrogen uptake in winter wheat by combining proximal crop measurements with Sentinel-2 and DMC satellite images in a decision support system for farmers. Acta Agric. Scand. Sect. B Soil Plant Sci 67, 637–650.
Söderström, M., Stadig, H., Nissen, K., Piikki, K., 2015. CropSAT: kväverekommendationer och grödstatuskartering inom fält genom en kombination av satellitdata och N-sensorer. Institutionen för mark och miljö, Sveriges lantbruksuniversitet (In Swedish).
Spörndly, R. (Ed.), 2003. Fodertabeller För Idisslare 2003. Sveriges lantbruksuniv.
Starke, A.R., Lemos, L.F., Boland, J., Cardemil, J.M., Colle, S., 2018. Resolution of the cloud enhancement problem for one-minute diffuse radiation prediction. Renew. Energy 125, 472–484.
Statistics Sweden, 2023. Electricity Supply and Use 2001–2021 (GWh). Available at: https://www.scb.se/en/finding-statistics/statistics-by-subject-area/energy/energy-supply-and-use/annual-energy-statistics-electricity-gas-and-district-heating/pong/tables-and-graphs/electricity-supply-and-use-20012021-gwh/. (Accessed 2 July 2023).
STICS, 2023. Simulateur mulTIdiciplinaire les Cutures Standard. Available at: https://www6.paca.inrae.fr/stics_eng/About-us. (Accessed 17 June 2023).
Strång. (2023). Available at: https://strang.smhi.se/. Accessed 4th October 2023.
Sturchio, M.A., Kannenberg, S.A., Knapp, A.K., 2024. Agrivoltaic arrays can maintain semi-arid grassland productivity and extend the seasonality of forage quality. Appl. Energy 356, 122418.
Sugimoto, H., 2001. Photosynthesis of daughter-tuber leaves in eddoe population and its contribution to Canopy photosynthesis and tuber yield. Jpn. J. Crop Sci. 70 (1), 92–98.
Sun, X., Khan, M.R., Deline, C., Alam, M.A., 2018. Optimization and performance of bifacial solar modules: a global perspective. Appl. Energy 212, 1601–1610.
Swedish Board of Agriculture, 2023. News in Agricultural Subsidies in 2023. Available at: https://jordbruksverket.se/stod/jordbruk-tradgard-och-rennaring/sam-ansokan-och-allmant-om-jordbrukarstoden/nyheter-i-jordbrukarstoden-2023. (Accessed 6 July 2023) (in Swedish).
The Swedish Government, 2000. Ds 2000:61 the Swedish Environmental Code.
Tidåker, P., Rosenqvist, H., Gunnarsson, C., Bergqvist, G., 2016. Räkna med vall – hur påverkas ekonomi och miljö när vall införs i spannmålsdominerade växtföljder? Rapport 445. In: Lantbruk & Industri, JTI – Institutet För Jordbruks Och Miljöteknik Uppsala.
Trommsdorff, M., Dhal, I.S., Özdemir, Ö.E., Ketzer, D., Weinberger, N., Rösch, C., 2022. Agrivoltaics: solar power generation and food production. In: Solar Energy Advancements in Agriculture and Food Production Systems. Academic Press, pp. 159–210.
Trommsdorff, M., Kang, J., Reise, C., Schindele, S., Bopp, G., Ehmann, A., et al., 2021. Combining food and energy production: design of an agrivoltaic system applied in arable and vegetable farming in Germany. Renew. Sustain. Energy Rev. 140, 110694.
Verheijen, F.G., Bastos, A.C., 2023. Discussion: avoid severe (future) soil erosion from agrivoltaics. Sci. Total Environ. 873, 162249.
Volden, H., Nielsen, N.I., 2011. Energy and metabolizable protein supply. In: Volden, H. (Ed.), NorFor – the Nordic Feed Evaluation System. Wageningen Academic Publishers, Wageningen, The Netherlands, pp. 81–84. EAAP publication No. 130.
Wang, Z., Ye, L., Jiang, J., Fan, Y., Zhang, X., 2022. Review of application of EPIC crop growth model. Ecol. Model. 467, 109952.
Weselek, A., Bauerle, A., Hartung, J., Zikeli, S., Lewandowski, I., Högy, P., 2021. Agrivoltaic system impacts on microclimate and yield of different crops within an organic crop rotation in a temperate climate. Agron. Sustain. Dev. 41 (5), 1–15.
Weselek, A., Ehmann, A., Zikeli, S., Lewandowski, I., Schindele, S., Högy, P., 2019. Agrophotovoltaic systems: applications, challenges, and opportunities. A review. Agronomy for Sustainable Development 39, 1–20.
Williams, J.R., Jones, C.A., Kiniry, J.R., Spanel, D.A., 1989. The EPIC crop growth model. Transactions of the ASAE 32 (2), 497–511.
Willockx, B., Lavaert, C., Cappelle, J., 2023. Performance evaluation of vertical bifacial and single-axis tracked agrivoltaic systems on arable land. Renew. Energy 217, 119181.
Wu, C., Liu, H., Yu, Y., Zhao, W., Liu, J., Yu, H., Yetemen, O., 2022. Ecohydrological Effects of Photovoltaic Solar Farms on Soil Microclimates and Moisture Regimes in Arid Northwest China: A Modeling Study, vol. 802. Science of The Total Environment, 149946.
Yajima, D., Toyoda, T., Kirimura, M., Araki, K., Ota, Y., Nishioka, K., 2023. Estimation model of agrivoltaic systems maximizing for both photovoltaic electricity generation and agricultural production. Energies 16 (7), 3261.

Zainali, S., Lu, S.M., Stridh, B., Avelin, A., Amaducci, S., Colauzzi, M., Campana, P.E., 2023b. Direct and diffuse shading factors modelling for the most representative agrivoltaic system layouts. Appl. Energy 339, 120981.

Zainali, S., Ma Lu, S., Potenza, E., Stridh, B., Avelin, A., Campana, P.E., 2023a. 3D view factor power output modelling of bifacial fixed, single, and dual-axis agrivoltaic systems. AgriVoltaics, 2023.

Zhao, C., Liu, B., Xiao, L., Hoogenboom, G., Boote, K.J., Kassie, B.T., et al., 2019. A SIMPLE crop model. Eur. J. Agron. 104, 97–106.